NASA Technical Memorandum 4350

Lightning Imaging Sensor (LIS) for the Earth Observing System

Hugh J. Christian, Richard J. Blakeslee,
and Steven J. Goodman

FEBRUARY 1992

NASA

NASA Technical Memorandum 4350

Lightning Imaging Sensor (LIS) for the Earth Observing System

Hugh J. Christian, Richard J. Blakeslee,
and Steven J. Goodman
George C. Marshall Space Flight Center
Marshall Space Flight Center, Alabama

National Aeronautics and
Space Administration
Office of Management
Scientific and Technical
Information Program
1992

PREFACE

This document describes scientific objectives and instrument characteristics of a calibrated optical Lightning Imaging Sensor (LIS) for the Earth Observing System (EOS) designed to acquire and investigate the distribution and variability of total lightning on a global basis. The LIS is an EOS instrument, whose lineage can be traced to a lightning mapper sensor planned for flight on the GOES series of operational meteorological satellites. The LIS is conceptually a simple device, consisting of a staring imager optimized to detect and locate lightning. The LIS will detect and locate lightning with storm scale resolution (i.e., 5-10 km) over a large region of the Earth's surface along the orbital track of the satellite, mark the time of occurrence of the lightning, and measure the radiant energy. The LIS will have a nearly uniform 90% detection efficiency within the area viewed by the sensor, and will detect intracloud and cloud-to-ground discharges during day and night conditions. In addition, the LIS will monitor individual storms and storm systems long enough (i.e., 2 minutes) to obtain a measure of the lightning flashing rate in these storms when they are within the field of view of the LIS. The LIS attributes include:

- **Low Cost**
- **Low Weight and Power (15 kg, 30 watts)**
- **Low Data Rate (6 kb/s)**
- **Important Science**

Lightning is one of the responses of the atmosphere to thermodynamic and dynamic forcing and, consequently, contains significant information about the atmosphere. Because of this information content, the LIS will provide unique global data sets, including:

- **Detection and Location of Deep Convection Without Land-Ocean Bias**
- **Estimation of Precipitation Mass in the Mixed Phased Region of Thunderclouds**
- **Differentiation of Storms with Strong Updrafts from Those with Weak Vertical Motions**
- **Information on Natural NO_x and Other Trace Gas Production in the Atmosphere**

Lightning measurements from an EOS satellite will contribute significantly to several important mission objectives. Lightning activity is closely coupled to storm convection, dynamics, and microphysics, and can be correlated to the global rates, amounts, and distribution of convective precipitation and to the release and transport of latent heat. These mesoscale phenomena influence and are influenced by global scale processes. The LIS will contribute to studies of the hydrological cycle, general circulation and sea-surface temperature variations, investigations of the electrical coupling of thunderstorms with the ionosphere and magnetosphere, and observations and modeling of the global electric circuit. It will provide a global lightning climatology from which changes, caused perhaps by subtle temperature variations, will be readily detected.

TABLE OF CONTENTS

LIST OF ILLUSTRATIONS

TECHNICAL MEMORANDUM

LIGHTNING IMAGING SENSOR (LIS) FOR THE EARTH OBSERVING SYSTEM (EOS)

I. INVESTIGATION AND TECHNICAL PLAN

A. INTRODUCTION

This document presents the scientific rationale for the flight of a calibrated optical Lightning Imaging Sensor (LIS) as part of the Earth Observing System (EOS). The addition of LIS would contribute to many of the goals and objectives of EOS. Lightning is an unique indicator of deep convection and is the only means presently available to detect deep convection from space without a land-ocean bias. It will also provide an early start for the development of a thunderstorm and lightning climatological data base. LIS is an EOS-A polar platform instrument, whose lineage can be traced to a lightning mapper sensor planned for flight on the GOES series of operational meteorological satellites. In this section, we discuss the lightning observations. We then briefly review previous observations of lightning from low-Earth orbit and establish the basis for making lightning measurements from space. This section is concluded by a description of the proposed lightning measurements and a discussion of synergisms with other EOS instruments.

1. The Need for Lightning Measurements in EOS

Lightning is a global phenomenon that can be used as a measure of some of the variables in global change. Lightning activity is associated with thunderstorms that produce heavy rainfall in many climatic regions and, therefore, can be used to increase our knowledge of the distribution, structure, and variability of thunderstorms at the local, regional, and global scale over the land and ocean. The world's major centers of organized mesoscale convection do not, in general, coincide with the 'maxima' in the thunderstorm day climatology. The orographic and environmental interactions that initiate and sustain long-lived convective activity yield a different, yet important, perspective that is difficult to appreciate when considering only the number of thunderstorm days. This occurs because thunderstorm day statistics tend to be dominated more by the diurnal cycle than by large scale dynamics and give equal weight both to a day in which perhaps only one lightning discharge occurs and to a day in which tens of thousands of discharges occur. For example, up to 25% of the entire annual lightning strikes at a given site within the Central U.S. can be accounted for by the passage of but a single mesoscale convective complex (Goodman and MacGorman, 1986).

Atmospheric teleconnections associated with naturally occurring climate variations such as ENSO (El Nino Southern Oscillation) and anti-ENSO events in the tropical Pacific often result in significant changes in the frequency and movement of storm tracks, precipitation patterns, and cloud cover. These climate variations will also produce changes in lightning activity in both the northern and southern hemispheres. Forest fires are often caused by lightning when the ground is dry, decayed vegetation is present, and surface winds are strong. Doubled CO_2 (i.e., global warming) climate simulations suggest a 25% increase in global lightning frequency (Price and Rind, 1990). Can we predict if naturally occurring forest fires (in northern boreal forests, in particular) will be more common in the future? Are global warming simulations of cloud amounts, distributions, and structures, limited by coarse model spatial resolution and relatively simple convective parameterizations, justified by the regional and global observations of

lightning? How might sub-cloud evaporation change? None of these questions can be answered without an improved, long-term observation capability.

The processes that lead to the production of lightning are tightly controlled by updraft activity and the formation of precipitation. Lightning seems to initiate soon after the onset of strong convection, after significant cloud mass and ice have formed in the upper regions of the thunderstorm. Lightning activity tends to track the updraft in both amplitude and phase with rates increasing as the updraft intensifies and decreasing rapidly with cessation of vertical growth. The charging process is dominate in the convective regions of the storm. It has been demonstrated that lightning observations from space will clearly delineate the regions of convection embedded within large stratiform cloud systems. Thus, the detection of lightning from space specifically identifies those regions that are of paramount importance in the rain formation process. This ability to uniquely identify and quantify the convective core regions of storm systems and the existence of a linear relationship between total rain volume and lightning flash rate (see section I.B.1) will make LIS an important addition to EOS. Lightning measurements are straightforward and produce small data sets for storage and analysis purposes. The LIS instrument will be a simple but important addition to the overall EOS objective.

2. Historic Perspective and Heritage

Historically, the electrification of thunderstorms and the resulting lightning have been studied on the smallest of scales in an attempt to understand the underlying physical principles that drive the processes. Observation and modeling studies have strongly intertwined cloud electrification, microphysics, and dynamics, resulting in important advances in our fundamental understanding with obvious needs for further clarification of the various process interactions and feedbacks involved. Recent measurements near Darwin, Australia during the monsoon and monsoon 'break' periods have revealed dramatic changes (factor of 10) in lightning frequency associated with modest variations in surface wet bulb temperature (Williams et al., 1991). Thunderstorm wind fields, precipitation and lightning are tightly coupled in time and space and lightning cannot occur without the others. That is, strong updrafts and precipitation are necessary but not sufficient conditions for the production of lightning. There is significant effort to quantify those interactions.

While lightning and thunderstorms occur on local and regional scales, their effects have global consequences. For example, deep convective storms in the tropics are believed to be an important mechanism for heat transport from the surface to the upper troposphere in the Intertropical Convergence Zone (ITCZ) and contribute energy to drive both Walker and Hadley cell circulations. Lightning has been observed from above clouds using sensors installed on airplanes (e.g., Christian et al., 1983), high altitude balloons (e.g., Holzworth and Chiu, 1982), and satellites (e.g., Turman, 1979). Airplanes are excellent platforms for making close-up, detailed measurements of lightning characteristics, and although aircraft can be vectored to specific regions of a cloud for coordinated studies of storms from above and below, it is not possible to obtain a global view using research aircraft. Nor can a global view be adequately obtained with high altitude balloon observations. Satellites, on the other hand, represent ideal platforms for investigating lightning activity on the global scale.

Over the past 25 years, more than a dozen Earth-orbiting spacecraft have flown instruments that have recorded signals from lightning. The OSO-2 (Vorpahl et al., 1970), OSO-5 (Sparrow and Ney, 1971), and DMSP (e.g., Turman, 1978; Turman and Tettelbach, 1980; Orville and Henderson, 1986) satellites observed lightning with various optical sensors. Lightning sferics have been measured by radio frequency (rf) sensors on the RAE-1 (Herman et al., 1965), ARIEL-3 (Horner and Bent, 1969), and the ISS-b (Kotaki and Katoh, 1983) satellites. The

shuttle-based Night/Day Optical Survey of Lightning (NOSL) (Vonnegut et al., 1983) used a small hand-held instrument package consisting of a 16 mm cine movie camera and a solar cell optical pulse detector and recorder, while the shuttle-based Mesoscale Lightning Experiment (MLE) used payload bay TV cameras to obtain video images of nighttime lightning activity over the Earth. The detection of lightning from some of these satellites was a primary research objective, while for others it was an unanticipated bonus. In general, however, the various instrument packages were unable to provide very precise information on the lightning characteristics, spatial extent, and discharge frequency. Also, the location accuracy tended to be poor (hundreds of kilometers) due to the low spatial resolution of the detectors and the detection efficiency of the systems was often less than 2%, resulting in severe undersampling of the worldwide lightning activity. Table 1 summarizes most of the lightning experiments that have been conducted from space, and compares them to the LIS and the proposed geostationary Lightning Mapper Sensor (LMS).

During the 1980's, extensive optical and electrical observations of lightning were made from a high altitude NASA U-2 airplane with the primary objective of defining a baseline design criteria for a space sensor capable of mapping lightning discharges from geostationary orbit during day and night with high spatial resolution and high detection efficiency. The results of the U-2 investigations, parametric trade-off studies, and other research (Thomason and Krider, 1982; Norwood, 1983; Eaton et al., 1983; Christian et al., 1984, 1989; Christian and Goodman, 1987; Goodman et al., 1988a) have clearly established the feasibility of making this kind of lightning measurement from space using present state-of-the-art technology. Based on this research, an economical optical lightning imaging sensor has been conceptually developed for deployment in low-Earth orbit for EOS. An overview of the the EOS-A LIS measurement approach and the characteristics of the cloud top lightning signals which would be observed from space are presented in section I.C.

3. Investigation Objectives

The overall investigation objectives of this instrument are, as stated earlier, to fly a calibrated optical Lightning Imaging Sensor (LIS) as part of EOS in order to acquire and investigate the distribution and variability of total lightning over the Earth, and to increase understanding of underlying and interrelated processes in the Earth/atmosphere system. The LIS will be particularly valuable in providing observations over the data-sparse oceans and tropical regions of the world. The proposed lightning measurements provided by the LIS will address primary science objectives which will not be made by any other for instruments. A number of scientific investigations that will employ the LIS measurements are outlined in section I.B.

In terms of measurement capabilities, the LIS will detect and locate lightning with storm scale resolution (i.e., <10 km) over a large region at the Earth's surface along the orbital track of the satellite, mark the time of occurrence of the lightning with 2 ms resolution, and measure the radiant energy. The LIS will have a nearly uniform 90% detection efficiency within the field of view of the sensor, and will detect intracloud and cloud-to-ground discharges during the day and night. The LIS will view a total area exceeding 1000 km × 1000 km at the cloud top using a 128 × 128 photodiode array. (For example, the entire globe will be covered by the EOS-A LIS instrument every 6 days.) The ground-track speed of 6.67 km s^{-1} allows the LIS to monitor individual storms and storm systems for minutes, a period long enough to obtain a good measure of the lightning flashing rate in these storms while the storm is in the field of view of the LIS. It will be possible to estimate lightning frequency even for storms with flash rates as low as 1-2 discharges per minute. In addition, as a result of the very high temporal resolution of the LIS (i.e., events marked to the nearest 2 ms), effects due to satellite motion can be

Table 1. Lightning Experiments from Space

Satellite/Spacecraft	Launch Date	Sensor	Altitude (km)	Period	Lightning Power Sensitivity (Watts)	Footprint
Optical						
OSO 2,5	1965, 1969	Photometers	600	Moonless Night	$\sim 10^{8}$	
VELA V	1970	Photodiodes	1.1×10^{5}	Day-Night	$10^{11} - 10^{13}$	Very Wide Field of View
DMSP	1970	Scanning Radiometer	830	Local Midnight	Sensitive	100 km
DMSP-SSL	1974	12 Photodiodes	830	Local Midnight	$10^{8} - 10^{10}$	700 km
DMSP-PBE 2,3	1977	2.5 mm Photodiode	830	Dawn/Dusk	$4 \times 10^{9} - 10^{13}$	1360 km
S81-1 (SEEP)	1982	Particle Spectrometer Airglow Photometers (391.4, 390.8, 630.3 nm)	230	Night	10 R	100 km
Space Shuttle-NOSL	1981-1983	Photocell Plus Film	150	Shuttle Flights STS-2, 4, 6	NA	Variable
Space Shuttle-MLE	1988-1990	Payload Bay Video Cameras	150	STS-26, 30, 32, 34	NA	Variable
RF						
ARIEL-3	1967	HF Radio Receivers 5, 10, 15 MHz	600	Day/Night	RF	"Iris" Effect
RAE-1	1968	HF Radio Receivers 0.2 - 9.18 MHz	5850			Ionosphere Structure Dependence
ISS-b	1978	HF Radio Receivers 2.5, 5, 10, 25 MHz	1100			Several Hundreds of Kilometers
Goes-Next Lightning Mapper Sensor (Proposed)	Late 1990's	CCD Array	Geostationary	Continuous Coverage	$10^{8} - 10^{11}$	10 km
EOS-A Lightning Imaging Sensor (Proposed)	Late 1990's	CCD Array	Low Earth Orbit	Continuous Coverage Within Field of View	$10^{8} - 10^{11}$	1000 km x 1000 km Field of View with 10 km Pixel Resolution

neglected since the satellite platform will travel a distance of only 15 m in the time between successive readouts of the photodiode array. This distance is three orders of magnitude below the 8 km spatial resolution of the LIS.

Finally, it is worth stressing that the LIS represents a significant advance over any previous satellite-borne lightning detector. Lightning observations from the LIS can be readily associated with the thunderstorms that produced them, and the detection of even a single discharge is significant and provides important information (e.g., storm location, precipitation estimates, storm height, the presence of ice, lightning frequency, electric current output, etc.). The earlier satellite-borne lightning instruments could provide only a relative global distribution of lightning of a strictly statistical nature which required collecting data for long periods of time before it could be meaningfully interpreted in terms of global distributions. It was not possible to determine the lightning frequency of a particular storm with the earlier instruments, nor, for that matter, to even associate an individual discharge with a particular storm.

4. Contributions to the EOS Objectives

LIS will provide data that will enhance the primary EOS science objective: "study the Earths energy and water cycles." Algorithms could be developed to investigate the electrical, microphysical, and kinematic properties of thunderstorms. It is hypothesized that the type (intracloud versus ground discharges) and frequency of lightning is intimately related to the microphysical (e.g., ice mass) and kinematic properties of thunderstorm systems and their environment (e.g., available buoyant energy). Recent evidence suggests that the lightning activity can provide empirical estimates or bound the range of values for some geophysical properties such as the convective rain flux and rain rate, the vertical structure and distribution of storm mass (convective), latent heating rates, and the number and distribution of thunderstorms (Goodman et al., 1988b, 1989; Buechler and Goodman, 1990; Williams and Rutledge, 1990; Goodman and Christian, 1992). The results of these studies provide much of the physical basis from which multi-sensor fusion (e.g., combined precipitation) algorithms can be developed.

Little or no climatological lightning measurements exist to study the relationships between total lightning activity and precipitation processes. Pre-mission activity using data acquired by the TRMM and ground-based sensors will be used to develop initial precipitation and cloud characterization algorithms. The active radar on TRMM will be invaluable for validating lightning/microwave precipitation algorithms that could then be applied over the 15 year EOS mission to investigate the seasonal and interannual characteristics of convective clouds. Ground-based systems capable of detecting, locating, and characterizing lightning activity will initially be used for process studies that will be augmented with existing ground-based radars (deployed during field programs and NEXRAD), raingage, satellite, and rawinsonde data when available (e.g., Cape Canaveral, Florida). U.S. composite radar (available from WSI, Inc.) and global Defense Meteorological Satellite Program imagery will be archived (by on-going funded programs) at MSFC to be used by the investigators in conjunction with data collected by existing lightning networks. The DMSP Block-5 F10 and planned F11 satellite, scheduled for launch in November 1991 will produce co-registered Special Sensor Microwave/Imager (SSM/I) and Optical Linescan System (OLS) 2.7 km visible and infrared digital data sets for process studies and algorithm development.

5. Synergism with Other EOS Instruments

Many methods have been developed to determine convective rainfall amounts remotely using visible, microwave, and/or infrared observations from space-borne sensors. Deficiencies

exist in these techniques (Barret and Martin, 1981). One problem is properly delineating the convective areas. A satellite measurement system that senses the amount of lightning (both intracloud and cloud-to-ground) produced by thunderstorms could be used to improve rainfall estimation. This new determination of satellite rainfall overcomes some of the drawbacks of current techniques. Presently, IR thresholding for rainfall estimates is contaminated by signals from cirrus clouds. Combining the IR with VIS data is only useful during the daylight. Using the life history of the cloud to estimate rainfall amounts is hampered by the uncertainty of cloud-top features. Microwave emission and scattering both have problems with their low spatial resolution along with ambiguities between rain water and cloud signals. For example, the location of active lightning areas could be used to delineate the convective areas used by visible and infrared estimation techniques (Goodman et al., 1988c) and indicate the relative amount of precipitation-sized ice. Another possibility would be to develop a technique for estimating convective rainfall based upon the amount of lightning produced by the storm. Livingston and Krider (1978), Williams (1985), Goodman and MacGorman (1986), and others have developed relationships (i.e., empirical algorithms) for lightning rates as a function of storm size, height, and duration. Finally, it should be noted that the LIS will continuously image a monochromatic cloud scene for greater than 1 minute. This measurement may provide useful low (8 km) resolution (stereo) imagery and bireflectance data (as the cloud enters and exists the field of view) as an augmentation to other EOS sensors.

B. PROPOSED INVESTIGATIONS AND ANALYSES

We are proposing to use the lightning data to study five major research topics of scientific importance. They are:

- o Provide information on the total rain volume and degree of convective activity in the core regions of tropical and extra-tropical storms and storm systems.

- o Global studies of the distribution of lightning and its relationship to storm microphysics and dynamics, dependence on regional climatic environments and their changes, its relationship to precipitation and cloud type, and the incorporation of these relationships into diagnostic and predictive models of global precipitation the general circulation and the hydrological cycle.

- o Development of a global lightning climatology in order to study the distribution and variability in lightning frequency as an indicator of the intensity of the Walker and Hadley circulations and assessing the impact of sea surface and land surface temperature changes on the distribution and intensity of thunderstorms.

- o Observational and modeling studies of the global electric circuit and the factors that cause it to change.

- o Studies on the production, distribution, and transport of trace gases attributed to lightning and determine the contribution (and the sources of variability) to the global amount of trace gases.

1. Global Lightning and Precipitation

Water plays an essential role in many Earth system processes and is a necessary ingredient for sustaining life and global productivity. Clouds not only produce beneficial rainfall, but they also play an important role in the atmospheric energy and radiation budget.

Precipitation is not only an important component of the water budget, it is an important factor in the storm electrification process. Our current understanding of the quantitative relationship between lightning activity and surface rainfall is limited to a few case studies conducted in Florida (Piepgrass et al., 1982), Arizona (Battan, 1967), Alabama (Goodman et al., 1988b), and the Midwest (Grosh, 1978). Even with this limited data set, several relationships have been discovered. Braham (1952) proposed that convective clouds producing less than 10^7 kg of rain are unlikely to produce any lightning. Piepgrass et al. (1982) proposed that when lightning is possible in a storm, there is almost a direct proportionality between the total rain volume and the number of flashes. In addition, a detailed examination of two storms revealed that the temporal evolution of rainfall and total lightning (CG and intracloud) was similar, but with a time lag between the rainfall and lightning flash rate maxima of 4 and 9 min. Grosh (1978) found a similar time lag between the total flash rate and rainfall rate maxima. It should be noted that these studies used data from rain gauge networks for precipitation amounts. Storms not ideally situated over rain gauges will result in undersampling of the rainfall. However, the exact relationship between total rainfall, the climatic environment, and lightning activity is not yet fully understood.

Workman and Reynolds (1949) and Reynolds and Brook (1956) were among the first to show that lightning and precipitation development in thunderstorms are closely related. They noted that lightning is a sufficient, but not necessary, condition for precipitation. They observed that electrification occurs when the radar echo indicates rapid vertical development. Thus electrical activity is an important indicator of rapid storm development and precipitation. Battan (1965) compared visual counts of lightning to ground with rain gauge measurements and found that both the area average rainfall and lightning frequency increase according to the number, size, and duration of the convective clouds. On heavy rain days he observed more than 50 times as many lightning events as on light rain days.

Using radar observations of Oklahoma storms, Kinzer (1974) found a correlation between CG lightning counts and radar derived rainfall. Similar results were found in the Tennessee Valley region by Goodman and Buechler (1990). Large amounts of rain can fall during convective events. For example, during the warm (growing) season, mesoscale convective weather events account for approximately 30-70% of the total rainfall (Fritsch et al., 1986). Goodman and MacGorman (1986) studied the CG lightning characteristics of organized mesoscale systems and found that the total rain volume and lightning activity peaked at the same time and surface rainfall maxima generally corresponded with lightning ground strike maxima (Figure 1). In addition, a single mesoscale convective complex could produce as much as 25% of the annual total ground flashes at a given location.

Studies of small isolated thunderstorms in the northeastern U.S. (Shackford, 1960), southeastern U.S. (Goodman et al., 1988b; 1989), and in Darwin, Australia (Williams and Rutledge, 1990) indicate that a link exists between the updraft strength and the amount and type of lightning activity. Storms with a large amount of mass near the -10 °C level (the level of the main negative charge region in the thunderstorm central dipole) produce more total lightning (yet fewer CG flashes) than when the mass is concentrated lower in the cloud. Figure 2 shows two contrasting storm structures during the monsoon and "break" periods during the Australia summer. The monsoon period is characterized by shallow reflectivity cores indicating a low concentration of graupel, rimed ice, and hail in the mixed-phase region (0 °C to -20 °C) impor-

LIGHTNING-RAINFALL RELATIONSHIPS FOR CONVECTIVE SYSTEMS

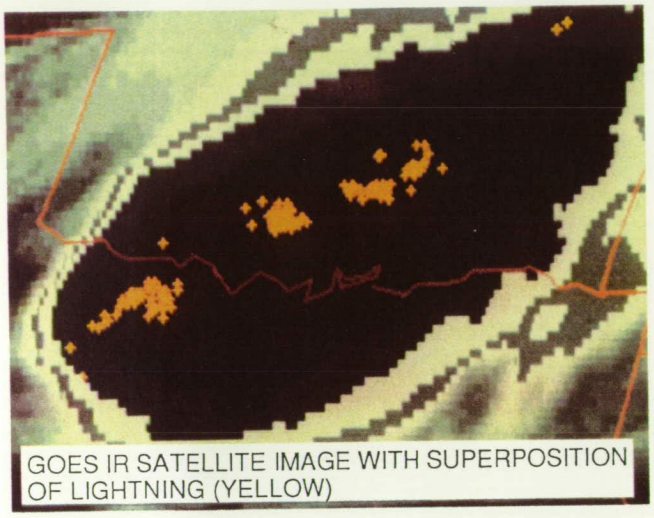

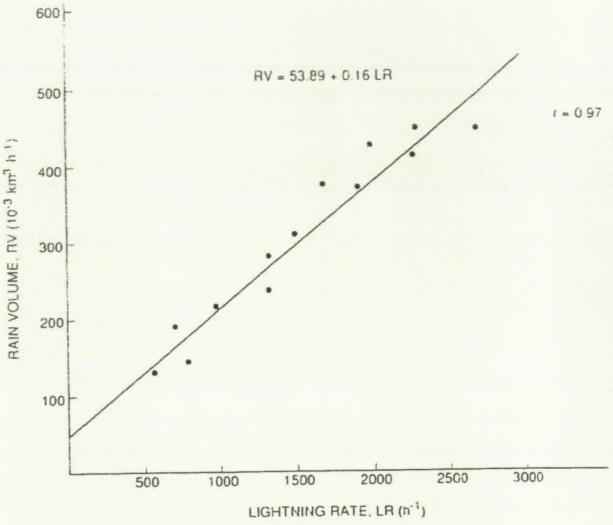

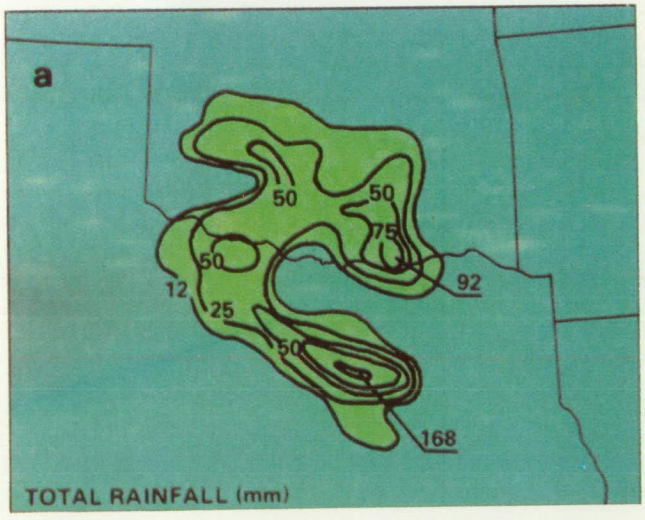

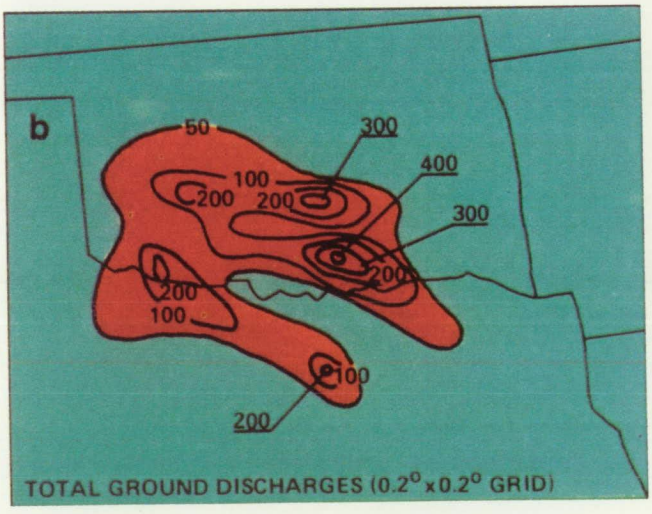

Fig. 1. Lightning-rainfall relationships for convective systems: Upper left, GOES infrared image (MB enhancement) of a mesoscale convective complex event on 13 June 1983 during the period of greatest hourly rainfall with lightning ground strikes (in yellow) superimposed; right, relationship between total rain volume and hourly cloud-to-ground discharge frequency for 10 mesoscale storm events; Lower left, contours of total gaged rainfall (> 12 mm) for the 13 June storm complex; lower right, contour plot of the total number of cloud-to-ground discharges produced by the 13 June storm complex (after Goodman and MacGorman, 1986).

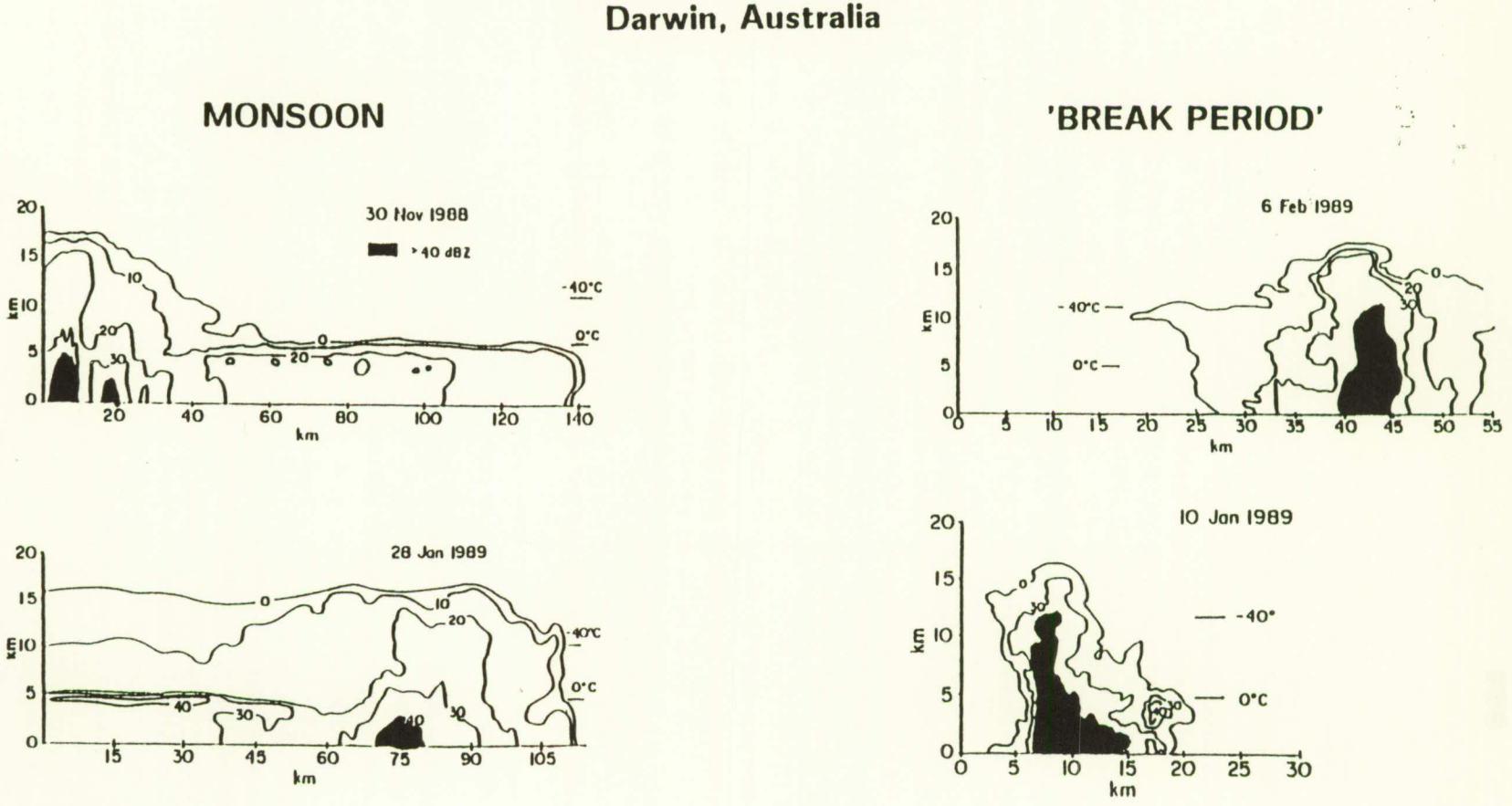

Fig. 2. Vertical cross-section of the reflectivity structure of thunderstorms in Darwin, Australia (after Williams et al., 1991).

tant for cloud electrification. Total lightning rates may only be a few flashes per minute. In contrast, the break period environment supports the convective "hot towers" that contain total flash rates of 40-60 per minute with more than 90% of all flashes in-cloud. Thus cloud-to-ground lightning rates alone can be an ambiguous indicator of the convective vigor of a storm. A similar result has been found in Alabama (Figure 3). Note that the first lightning (intracloud) flash occurs when the storm mass reaches 10^7 kg, a threshold first identified during the Thunderstorm Project (Byers and Braham, 1949), and the total flash rate is in-phase with the growth and decay of the storm. A comparison of the 10 January Darwin storm (peak flash rate of 60 min^{-1}) with the Huntsville storm (peak flash rate of 23 min^{-1}) indicates both produced approximately the same peak (radar-estimated) rain flux of 1-2 x 10^5 kg s^{-1}. Peak updraft speeds of 35 m s^{-1} and 25 m s^{-1}, respectively, were estimated by Doppler radars for the Darwin and the Huntsville storm. However, the precipitation-filled volume (Z>30 dBZ) of the Darwin storm was 500 km^3, nearly 2.5 times the volume of the Huntsville storm. Energy budget studies of air mass storms in Huntsville, AL also suggest the total lightning rates are proportional to the latent heating rates (Goodman et al., 1989).

We hypothesize that a stronger updraft allows more mass to reach greater altitudes where more frequent small particle interactions in a mixed phase region may play an important role in charge separation leading to enhanced overall lightning activity, and leads to a greater ratio of intracloud to CG discharges. Buechler and Goodman (1990) showed that peak 10 min CG rates are highly correlated to the maximum rain flux, yet the average rain volume per ground discharge decreases as the buoyancy increases. Zawadzki et al. (1981) found that environments supportive of strong updrafts have higher maximum rain rates. In general then, a stronger updraft should produce both more lightning and more intense surface rainfall. We suspect that the strength of the updraft is the primary reason that thunderstorms over land produce a factor of 10 more lightnings than storms over the ocean.

We propose to test these relationships in the tropics by analyzing LIS data in conjunction with the other EOS and TRMM sensors, and by comparing LIS observations with ground truth rainfall data sets.

2. Tropical Convection and Sea Surface Temperatures

One of the important links in the global atmospheric circulation research is the transport of heat from the tropics to the atmosphere and to higher latitudes. Most of the heat generated at the surface in the tropics is transported to the upper troposphere by deep convective tropical storms with much of the convection occurring in the Inter-Tropical Convergence Zone (ITCZ), a region of weak air currents having a net upward vertical motion leading to the formation of heavy clouds and rain. Although this convective energy transport is an important link in the total global circulation and these storms may constitute a significant fraction of the total number of thunderstorms, very little is known about the heat balance and numbers of these storms (Houze and Betts, 1981). Lightning frequency variations as a function of latitude show a December-February (northern hemisphere winter) peak of activity between 10° and 20°S and a June-August (northern hemisphere summer) peak between 10° and 20°N. (Turman, 1978). These variations tend to track the seasonal migration of the ITCZ. The ITCZ migrates as far as 15° north and south of the equator, reaching its northern most point in September and southern most in March, also corresponding to the seasons of highest temperatures in the oceans (Byers, 1974).

It is generally believed that heat transport from the surface to the upper troposphere in the ITCZ is through pseudoadiabatic ascent in the cores of large cumulonimbus clouds ("hot towers"). Heat balance in the equatorial zone can then be qualitatively accounted for if the ver-

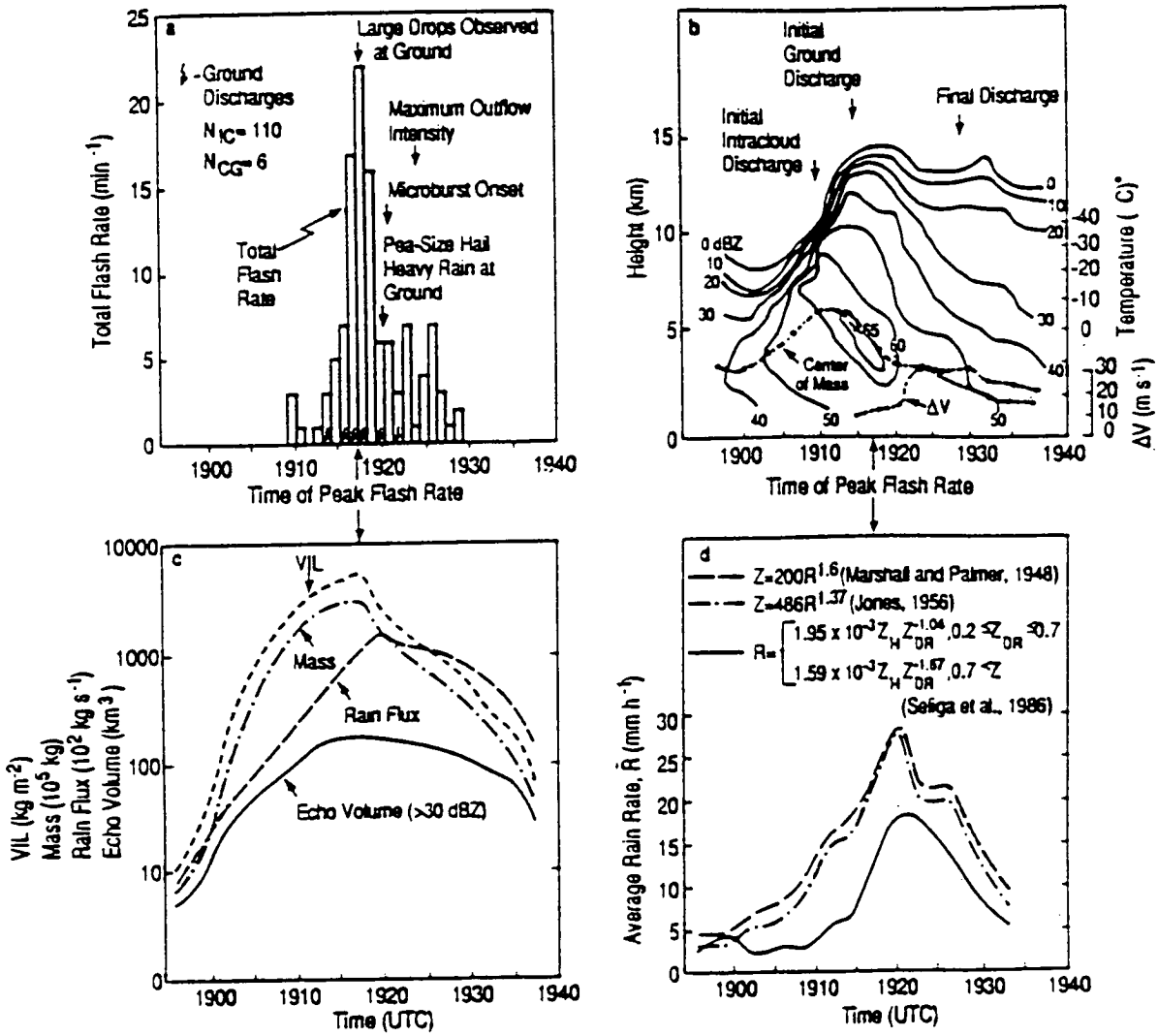

Fig. 3. Time-series of lightning activity and precipitation history for an air mass thunderstorm observed in Huntsville, AL (after Goodman et al., 1988b).

tical motion in the ITCZ is confined primarily to the updrafts of individual convective cells (Holton, 1972). Riehl and Malkus (1958) have estimated that 1500-5000 "hot towers" would need to exist simultaneously around the globe to account for the required vertical heat transport in the ITCZ; however, few attempts at verification have been made. The primary reason for the lack of study is that most of the deep convection in the tropics occurs over ocean areas where observing systems are inadequate at best (Houze and Betts, 1981; Robertson et al., 1984).

One way to alleviate the lack of data on tropical convection is to document the deep convection by the lightning it produces. Although most lightning studies have been made in temperate regions, storms in the tropics exhibit many of the features considered important for the production of lightning, such as strong convection above the freezing level, high rain rates, and forcing due to enhanced surface convergence (Robertson et al., 1984). Lightning should clearly delineate those deep oceanic storms with frozen precipitation particles aloft.

One long standing issue involves the processes responsible for maintaining the precipitation (heating) centers and convergence zones. There is considerable evidence linking warm sea surface temperature (SST) anomalies with precipitation maxima (Bjerknes, 1969; Cornejo-Garrido and Stone, 1977; Rasmussen and Carpenter, 1982). A preliminary analysis (performed by E. Williams) of two monsoon episodes at Darwin, Australia showed SST maxima and subsequent SST decreases of 1-1.5°C over a large area north of Australia associated with the monsoon convection which subsequently moved over the Australian continent. In light of an earlier result (Williams et al., 1991) that 1° of wet bulb temperature is equivalent to roughly 1000 J kg^{-1} of available buoyant energy, these short period changes are significant for storm and atmospheric energetics. The mechanisms by which this apparent linkage between surface forcing and atmospheric response occurs are generally in dispute. Neelin and Held (1987), for example, have found that precipitation is primarily balanced by moisture convergence rather than evaporation alone. Neelin and Held have argued that horizontal structure in the large scale moist static stability field is quite sensitive to SST and provides, in turn, a powerful constraint on tropical convergence. Lindzen and Nigam (1987) appeal strictly to the mass field gradients arising from SST forcing and a well mixed planetary boundary layer as a means of maintaining the convergence. In this scenario the direct effect of latent heat release is not important.

The relative distributions of lightning over the Earth at particular times of the day have been derived from earlier satellite measurements. Figure 4 shows the midnight lightning locations derived from DMSP Optical Linescan System (OLS) satellite data for winter and summer (Orville and Henderson, 1986). The primary regions of convective activity occurring over the Earth are clearly depicted in these maps. Note particularly that the lightning maps clearly show the seasonal shift of the inter-tropical convergence zone (ITCZ) from north of the equator in the northern hemisphere summer to south of the equator in the winter. Chen (1987) notes that the lightning activity in these maps is exactly where one would expect based on the convergence of water vapor brought about by planetary-scale divergent circulations. For example, in the tropics, local Hadley cell and east-west Walker circulations concentrate the precipitable water (and the upward vertical motions) over the three tropical continents in the same regions where Figure 4 shows the highest occurrence of lightning. Lightning occurrences in the extratropical regions, such as the peak in the summer northern hemisphere, also correspond well with planetary scale circulations and moisture transport leading to intense cyclonic activity accompanied by cumulus convection.

Figure 5 shows the DMSP midnight lightning activity (Goodman and Christian, 1992) and tropical rainfall (Janowiak and Arkin, 1990) for May 1987. The lightning maxima over the continents correspond to the rainfall maxima suggesting that land-based thunderstorms are major contributors to tropical continental rainfall. Due to a lack of geostationary satellite data and less favorable equator crossing times for the NOAA polar orbiting satellites used to produce

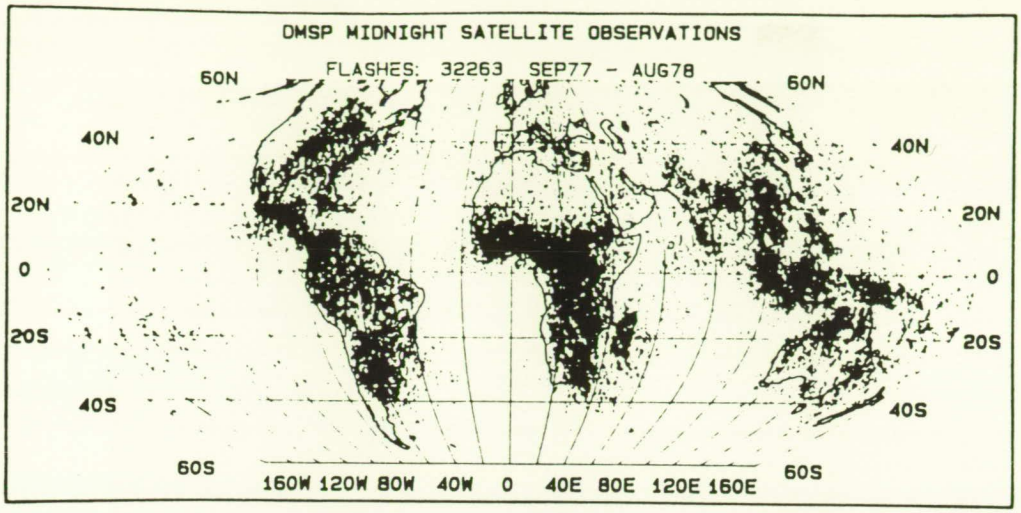

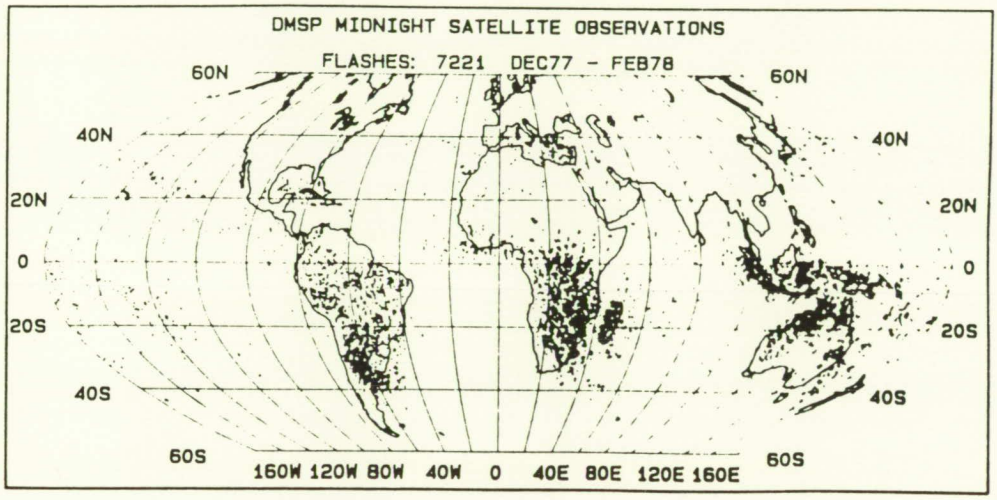

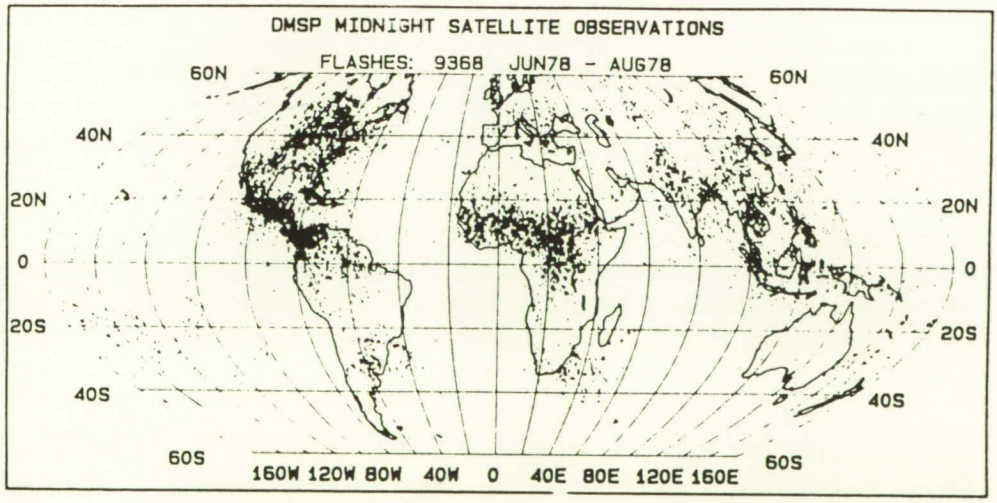

Fig. 4. Top, one year of DMSP-OLS midnight lightning discharges for 365 consecutive days for the period September 1977 to August 1978; Middle, DMSP-OLS midnight lightning for the N. hemisphere winter December 1977 to February 1978; Bottom, DMSP-OLS midnight lightning for the N. hemisphere summer June-August 1978 (after Orville and Henderson, 1986).

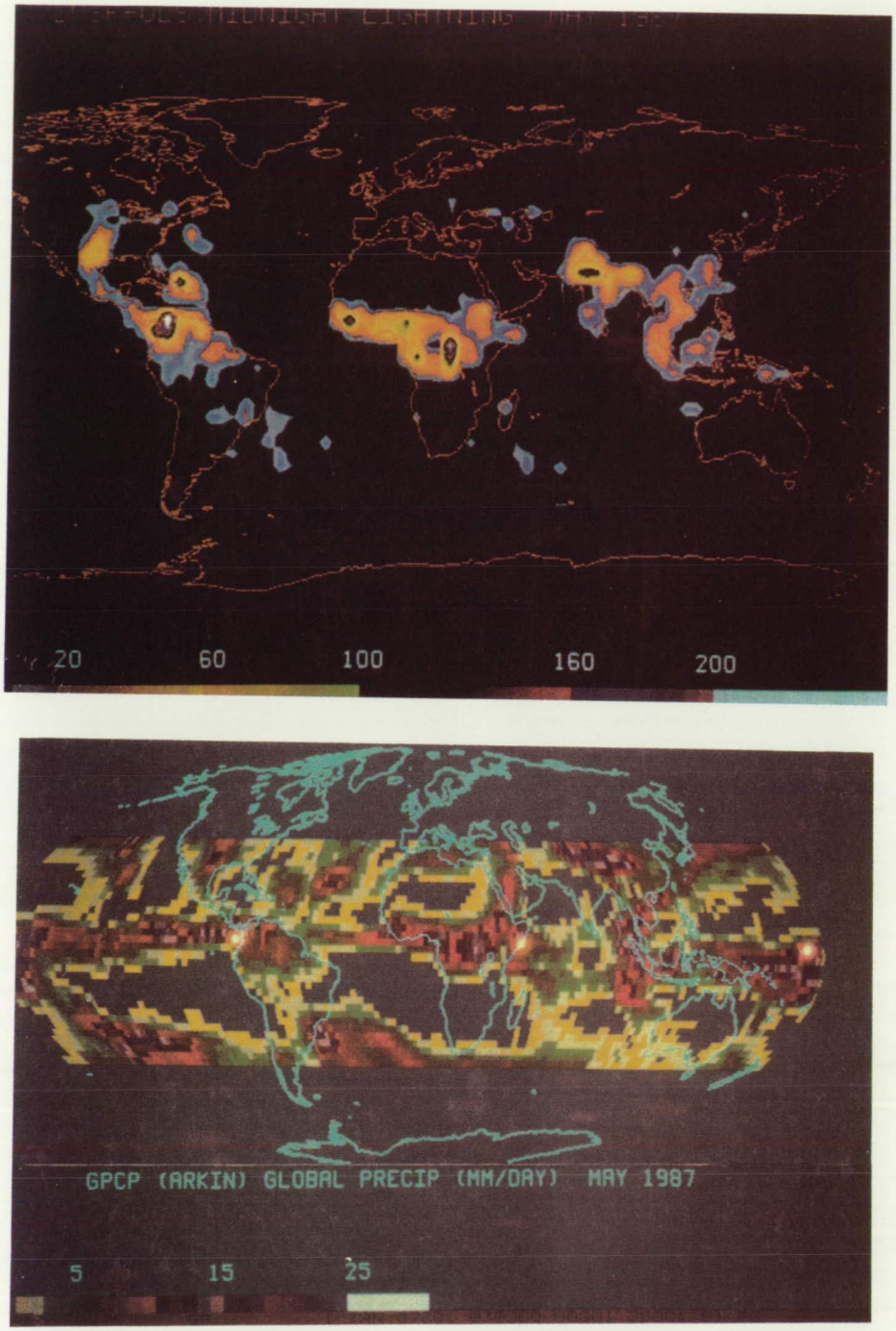

Fig. 5. Top, midnight lightning observed by the visible channel of the DMSP F9 OLS for May 1987 (units in number of lightning flashes within a 4^{o} latitude x 4^{o} longitude bin) (after Goodman and Christian, 1992). Bottom, global precipitation index from infrared channel of GOES geostationary and NOAA polar orbiting satellites for May 1987 (units of mm/day) (after Janowiak and Arkin, 1990).

this rainfall product for the Global Precipitation Climatology Project, the midnight thunderstorm (i.e., lightning) maxima over the Indian sub-continent and Pakistan seen by the DMSP OLS is not reflected in the GPCP rainfall product.

The diabatic heating maxima shown in Figure 6 for May 1987 supports the notion that latent heating due to thunderstorms and long-lived mesoscale convective systems that persist late in the evening over the tropical continents is a major source of tropical energetics. On the other hand the lightning and rainfall maps in the vicinity of southern Brazil and northern Argentina correspond to a major storm track in the Atlantic that is not revealed by the heating field diagnosed from the ECMWF analysis in the Atlantic. It is believed that this inconsistency is due to an absence of upper air information in this region.

There are other aspects of tropical meteorology that can benefit from the global distribution of lightning. These include the significant intraseasonal variability in tropical forcing (diabatic) and the somewhat vague relationship between this forcing and changes in the mid-latitude circulation. Knowledge of the variability in tropical precipitation, via the LIS sensor, would help resolve the temporal and spatial scales of the variability in tropical forcing. Once general relationships between lightning, the mechanisms that determine deep tropical convection, and sea surface temperatures are established from ground and satellite observations, the mechanisms that determine the amount and distribution of deep tropical convection can be addressed.

The above discussion strongly demonstrates the great potential that lightning measurements would provide to studies of the hydrologic cycle, atmospheric circulation, worldwide precipitation, and other EOS investigations. However, it should also be recognized that the previous generation satellite-borne lightning detectors are unable to provide the type of quantitative data sets required for EOS science. Research and development efforts in recent years have led to the design of an advanced lightning imaging sensor which offers storm scale spatial resolution and high detection efficiency, and which should be given serious consideration for inclusion as part of the total complement of scientific instruments flown on the platform.

In summary, the lightning distributions reflect regions of strong convective activity over the Earth without land ocean bias, provide important insights on the planetary-scale circulations, and can be used to generate consistency between data products to produce an optimal diagnosis of atmospheric processes.

3. Rainfall Estimates from Geostationary Orbit

An EOS sensor complement of MIMR, MODIS and LIS offers an opportunity to evaluate the lightning/storm structure/rainfall relationships that could be employed when a geostationary lightning mapper collects data simultaneously with only visible and infrared sensors on GOES-Next (Christian et al., 1989). The baseline EOS rainfall estimates will depend only on passive microwave measurements, augmented by VIS/IR data to confirm the presence of clouds, their height, etc. An important application of EOS VIS/IR data will be to bridge the system's rain estimate capabilities with the temporally resolved geosynchronous rain estimates which are presently inferred from only VIS/IR observations. Because of the short duration and high temporal variability of many precipitation events, geosynchronous rain observations remain of paramount importance. In the same manner that it is anticipated that simultaneous microwave measurements will lead to improved VIS/IR rain retrieval algorithms, the addition of LIS to EOS will allow intercomparison between lightning flash rates, microwave and VIS/IR imaging, leading to improved quantification of lightning-rainfall relationships (Figure 7). Better understanding of how to use lightning data in conjunction with VIS/IR imaging should profoundly affect our ability to make rainfall estimations from geostationary orbits.

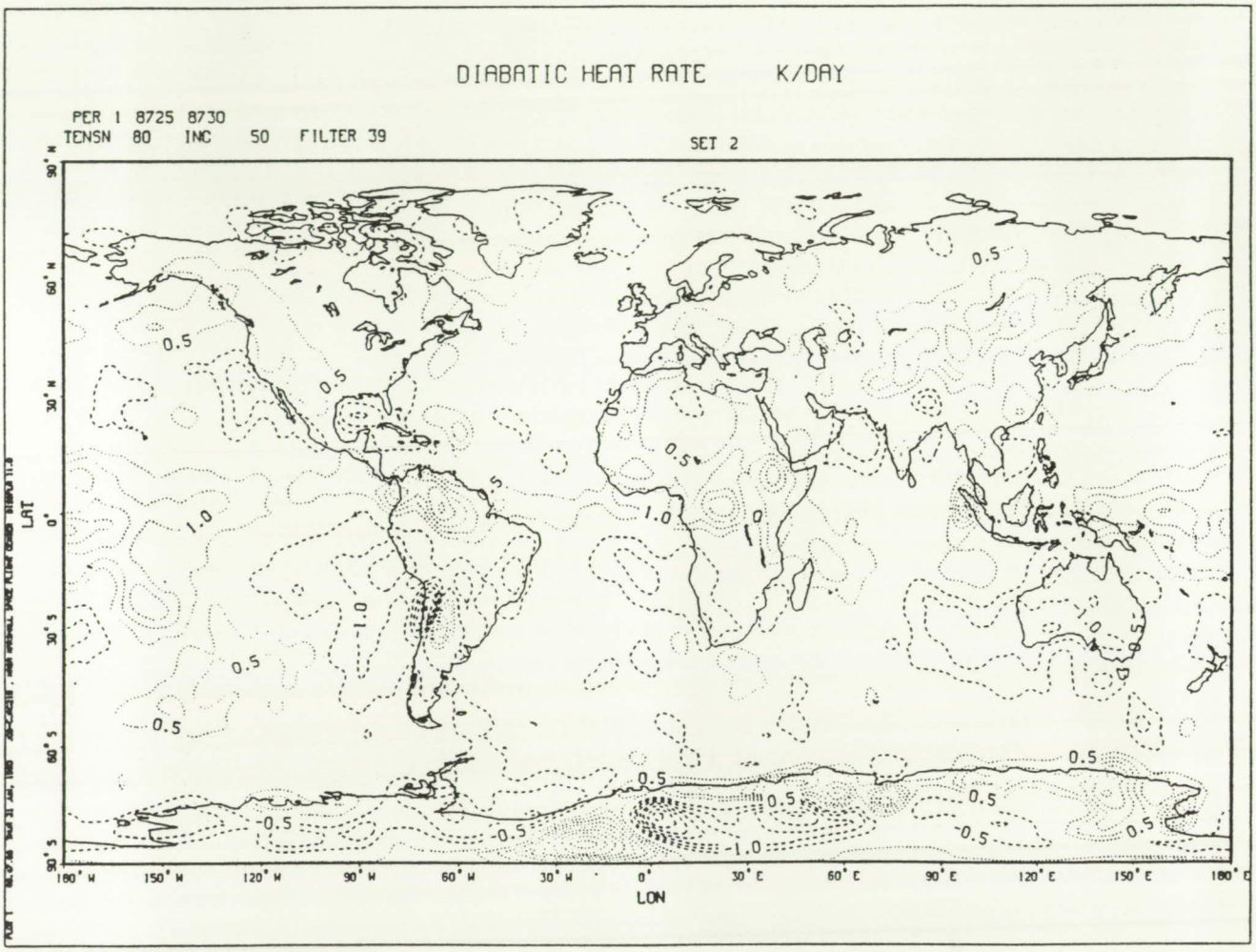

Fig. 6. Vertically integrated diabatic heating rate calculated from the residual of the dry thermodynamic equation from 7 level, 2.5° gridded ECMWF analysis for May 1987 (Christy, 1991). Values are in °K/day determined for the layer from the surface pressure level to 50 hPa. Contour interval is every 0.5 °K/day with positive values dotted, negative values dashed.

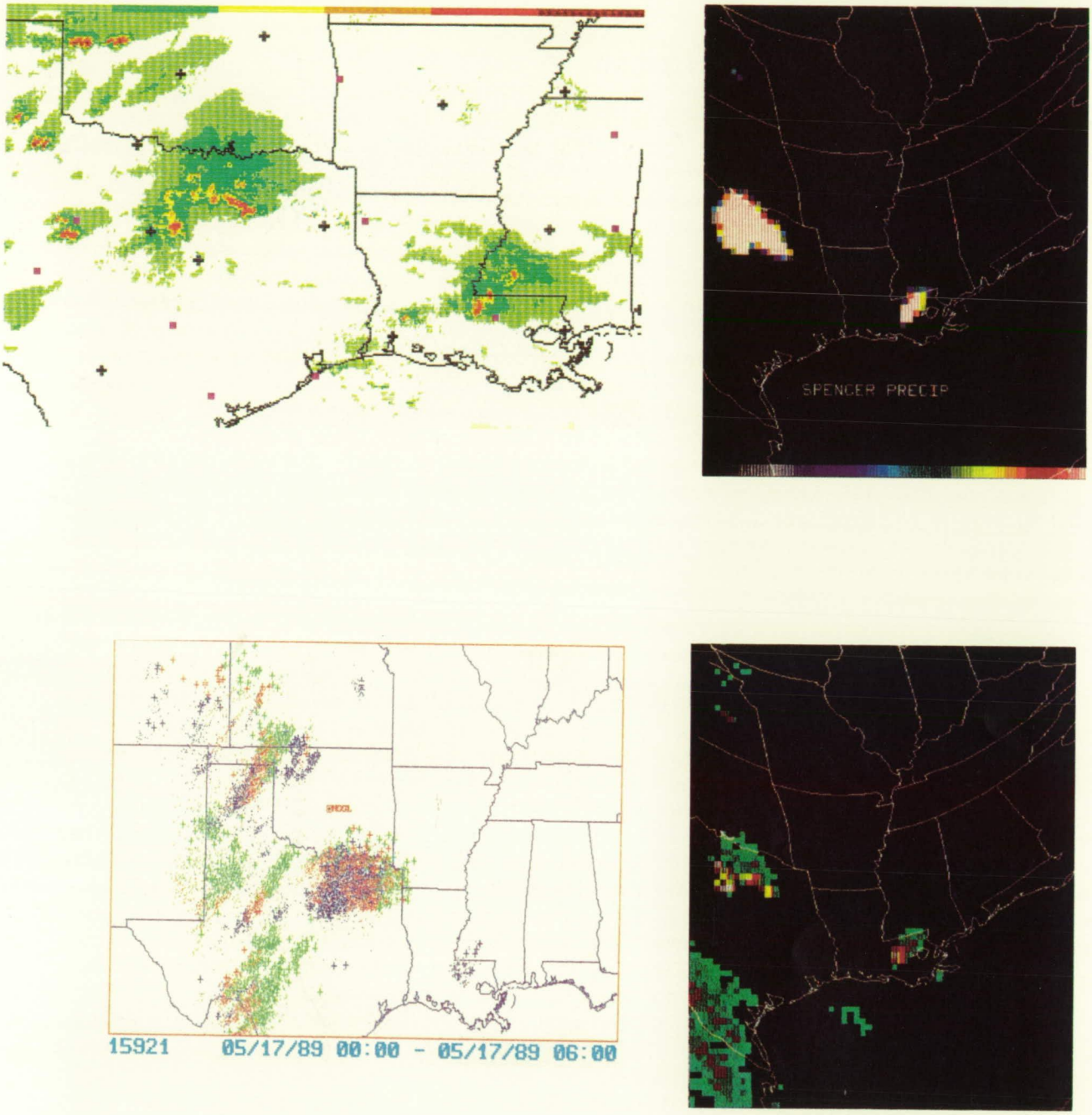

Fig. 7. Lightning and precipitation structure of a mesoscale convective system in the southern U.S. observed on 17 May 1989 by weather radar network (upper left), lightning ground strike network (lower left) and the DMSP F8 SSM/I passive microwave sensor (upper and lower right). The radar shows VIP level intensities 1-6 from a (WSI, Inc.) regional radar composite at 0100 UTC. The lightning strikes are shown during the 6-h period 0000-0600 UTC with color changes (purple, red, green) every 2 h. SSM/I rainfall products. Upper right, precipitating clouds (R. Spencer algorithm, personnel communication). Lower right, rain rate (Olson et al., 1990). From the 0100 UTC pass of the F8 satellite.

Plans are presently underway to add a lightning mapper sensor (LMS), an enhanced version of LIS, to a GOES satellite. When this occurs, the synergies between lightning and VIS/IR information could be exploited in order to provide improved time-resolved rainfall estimates. It can be anticipated that there will be a significant period during which only lightning-VIS/IR data will be available for geostationary orbit. Even when passive microwave measurements become available on future geostationary platforms, their spatial resolution at the lower frequencies of interest may be insufficient to resolve the convective cores of many storms.

Lightning and VIS/IR measurements should be very complementary. Lightning is primarily produced in the strong convective regions of a storm by processes occurring deep within the heart of the cloud. VIS/IR images, on the other hand, while providing only cloud top information are invaluable in identifying stratiform rain regions, an area where lightning sensors have little to contribute. As discussed previously, lightning activity closely follows convective activity, increasing as the storm intensifies and decreasing rapidly as the storm decays. Various investigations have demonstrated that the cold cloud top canopy, as viewed in IR, appears to continue to grow long after a cloud has entered its dissipation stage, thus producing errors in IR derived rainfall estimates. The addition of lightning data will clearly delineate the life of the storm and eliminate this source of error. As a final example, Williams et al. (1990) discusses what appears to be significant differences in the lightning activity associated with tropical monsoonal storms and tropical continental storms, thus combining lightning with VIS/IR should lead to accurate storm type identification and the application of an appropriate rainfall estimation algorithm.

4. Global Electric Circuit and Lightning Climatology

During fair weather conditions, there is a potential difference of 200 to 500 kV between the ionosphere and the Earth and a fair weather current of about 2 pA m^{-2} flows between the ionosphere and the Earth. Wilson (1920) proposed that this potential difference between the Earth and ionosphere is maintained by the world-wide distribution of thunderstorms. Present thunderstorm measurements and theories indicate that, on the average, each thunderstorm generates about 1 A of current that flows into the stratosphere. To maintain the fair weather global electric current flowing to the Earth, about 1000 to 2000 thunderstorms must to be active at any given time. Although the theory that thunderstorms are responsible for the ionospheric potential and fair weather atmospheric current is widely accepted in the atmospheric community, the details have not been proven. Previous attempts to study the global electric circuit have relied on ground-based radio frequency measurements of the global thunderstorm rate. These measurements have very significant uncertainties associated with them.

A lightning sensor on the polar platform would help alleviate some of the uncertainties in the global thunderstorm activity level. The optical measurements of the lightning activity would not only enhance ground-based measurements, but would also be a direct measure of the global thunderstorm rate. Over a period of years, the data set from the polar lightning sensor would produce an accurate estimate of the global flash rate. A recent study (Blakeslee et al., 1989) found a linear relationship between the total flash rate of a thunderstorm and the current produced by the thunderstorm (Figure 8). Once the global thunderstorm activity level and thunderstorm current are known, the results would provide for a definite test of the present theory on the global electric circuit and the means to monitor the global circuit via the global lightning flashing rate obtain from the LIS data.

One potential source for lightning distribution studies are ground-based lightning networks. These networks, however, have major disadvantages, including the fact that their coverage is limited to a few sections of the globe and their detection efficiency is less than 75% (Mach et

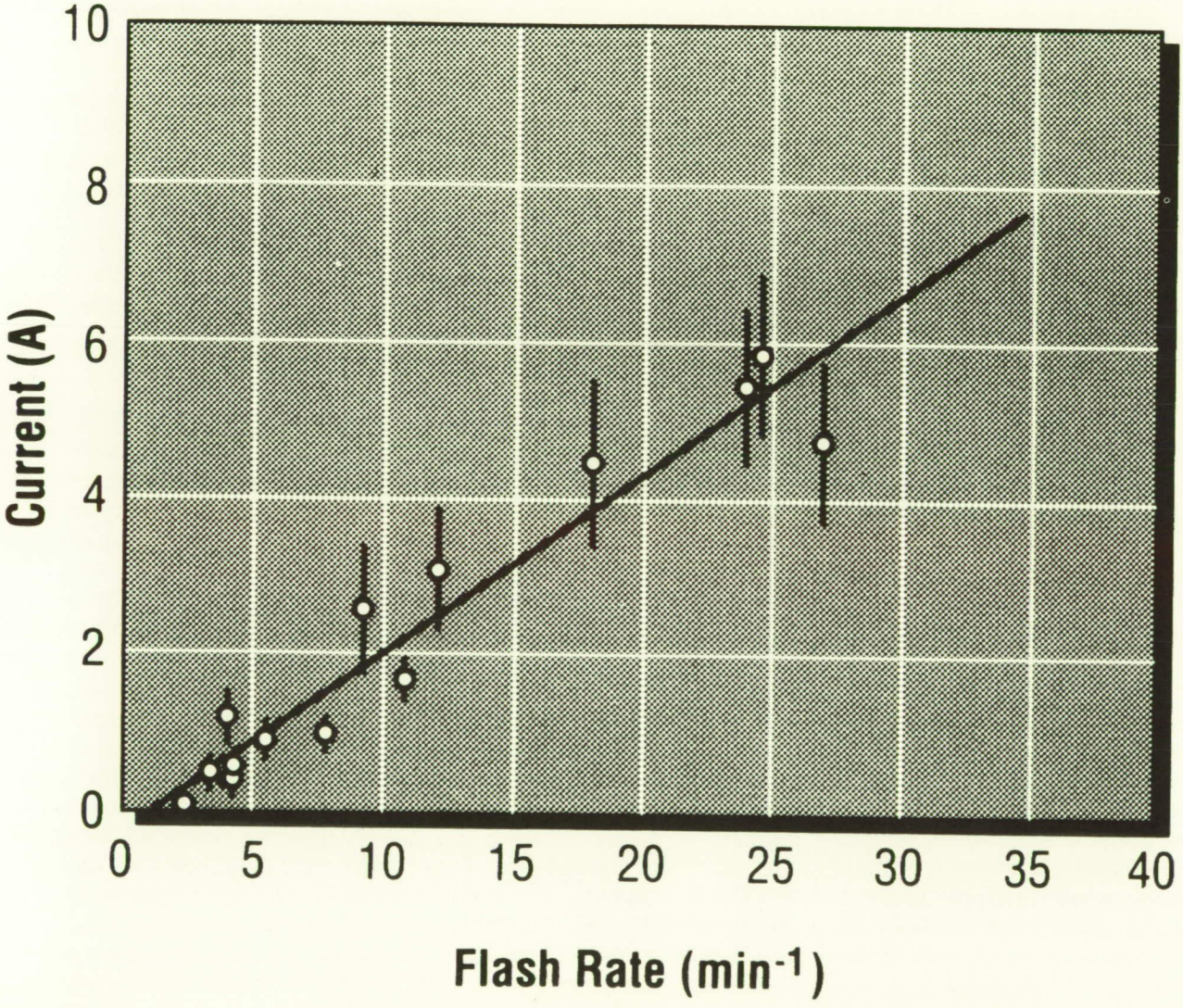

Fig. 8. Linear relationship between the total flash rate of a thunderstorm and the current produced by the thunderstorm.

al., 1986). In addition, the ground-based networks detect only cloud-to-ground lightning missing intracloud lightning which constitute the majority of all lightning discharges. To obtain a true measure of the global lightning flash rate, all lightning must be detected with a high detection efficiency. An orbiting optical lightning sensor provides the best means for accomplishing these goals for determining the total global lightning distribution.

Presently, an important source for global lightning distributions has been polar satellite sensors (e.g., DMSP/OLS), but as has been noted in section I.A.2, these sensors have several serious limitations. The spatial resolution of the highest resolution sensor was no better than 100 km, thereby missing important smaller scale features, and the satellite systems were unable to relate the lightning event with the parent storm system. Finally, the detection efficiency of previous sensors was often on the order of 2% or less. Estimating the total global lightning distribution for a year from these data results in large uncertainties and is probably not feasible.

With the proposed polar lightning sensor, each storm observed by the LIS will be sampled continuously for almost 3 minutes with very high detection efficiency. This will allow a statistically meaningful global lightning rate to be produced. Once a climatology of global lightning activity has been developed, we will then be able to apply LIS data for indications of global change. As noted previously, we anticipate that very small changes in sea surface and land surface temperature will produce large changes in the frequency and distribution of lightning. The order-of-magnitude increase in spatial resolution and detection efficient will also produce detailed results unattainable with previous studies (e.g., determining accurate "snap shot" or instantaneous flash rates for individual storms or storm complexes).

5. Atmospheric Chemistry Processes

The very high temperatures generated by lightning discharges and the subsequent rapid cooling rates of the lightning channels can significantly alter the chemical composition of certain trace gases in the atmosphere. Concentrations of trace constituents increase substantially in the high temperature lightning plasma when the chemical reaction rates and associated equilibrium levels are high. As the channel rapidly cools, trace species are "frozen-out" at levels well above the ambient equilibrium concentrations because the reaction rates are lowered to much slower values preventing the quick return of the newly raised trace gas concentrations to ambient background levels.

There is strong evidence that lightning is an important, though probably not the dominant, source of odd nitrogen in the Earth's atmosphere. However, lightning may be a dominant source of the nitrogen fixed in the upper regions of tall thunderstorms where it could conceivably be transported into the stratosphere. If the nitrogen fixed by lightning in the upper parts of thunderstorms does reach the stratosphere, then lightning may be a major source of stratospheric NO_x where it could interact with stratospheric ozone. During the fall 1983 airborne field operation of the NASA Global Tropospheric Experiment (GTE) Chemical Instrumentation Test and Evaluation (CITE-1) program, NO levels were observed to change from a background level of about 20 parts per trillion per volume (pptv) to levels approaching 1000 pptv during penetrations of two cumulonimbus anvils providing strong circumstantial evidence for a sizable source of NO in thunderclouds (Chameides et al., 1987). These results are shown in Figure 9. In the study, good agreement was found between the laser-induced fluorescence (LIF) system and two chemiluminescence (CL) systems employed to measure NO.

A number of other studies have found evidence of enhanced levels of NO and NO_2 in the vicinity of active thunderstorms (e.g., Noxon, 1976, 1978; Drapcho et al., 1983; Levine and Shaw, 1983; Franzblau and Popp, 1989). Further, recent studies (e.g., Christian and Goodman, 1987) have shown that a great deal of lightning occurs in the upper portions of thunderclouds

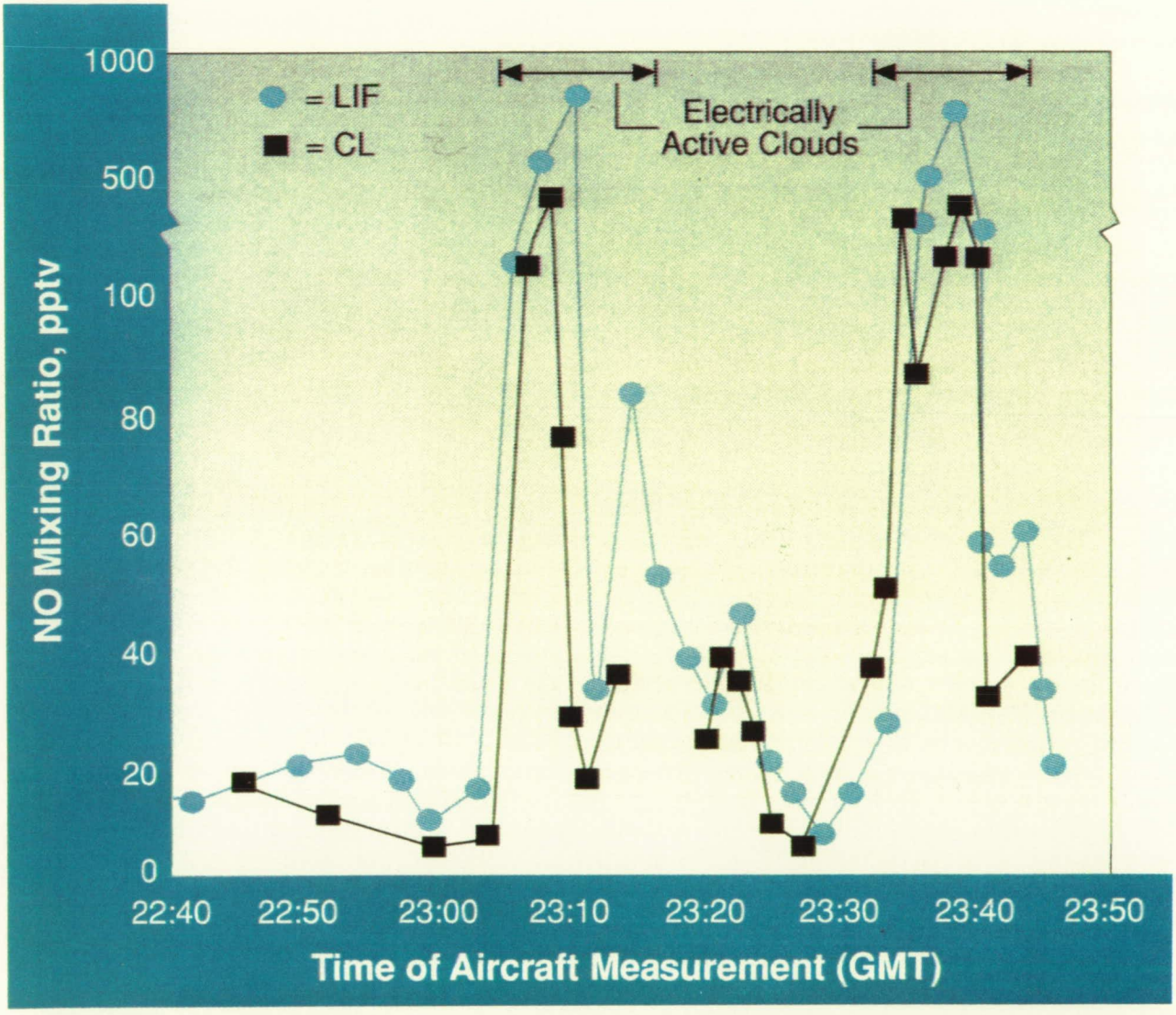

Fig. 9. Production of NO by lightning within clouds in the tropical Pacific during CITE-1 (after NASA Pub. - Global Tropospheric Experiment, Probing the Chemistry/Climate Connection, 1990).

and generally in the updraft regions, providing an effective mechanism for transporting NO_x across the tropopause into the lower stratosphere.

The relative importance of lightning as a natural source of NO_x has not been quantified in either the production efficiency of NO_x on a per flash basis or in an accurate determination based on total lightning rates on a global basis. Present estimates indicate that lightning fixes from 0.8 - 90 x 10^{12} g of nitrogen per year (Chameides, 1986). The wide range in these estimates reflects uncertainties in the physical characteristics of in-cloud lightning and in the total amount of lightning occurring at any time worldwide. Present consensus seems to be that lightning is an important (perhaps dominant) natural source of NO_x but that anthropogenic sources dominate. The uncertainty levels, however, are so large that further investigations are required.

C. LIS CONCEPTS/CAPABILITIES

The Lightning Imaging Sensor will detect and locate lightning with storm scale resolution (i.e., ~10 km) over a large region at the Earth's surface along the orbital track of the satellite, mark the time of occurrence of the lightning, and measure the radiant energy. The LIS instrument will detect intracloud and cloud-to-ground discharges during daytime and nighttime conditions. This section briefly describes lightning signal characteristics, particularly the characteristics of cloud top optical signals, discusses the basic LIS measurement approach, and finally summarizes the characteristics and capabilities of the LIS.

1. Lightning Signal Characteristics

The occurrence of lightning is accompanied by the sudden release of electrical energy which is converted into rapid heating in the vicinity of the lightning channel, the generation of a shock wave (which rapidly decays into an acoustic wave, i.e., thunder), and electromagnetic radiation ranging from extremely low frequency (ELF) radio waves to x-rays. One of the strongest radiation regions is in the optical wavelengths with peak power typically between 100 to 1000 MW. These optical emissions result from the dissociation, excitation, and subsequent recombination of atmospheric constituents as they respond to the sudden heating in the lightning channel. The heating is so intense (electron temperatures > 20,000 K) that the optical emissions occur primarily at discrete atomic lines with some continuum at shorter wavelengths. Measurements from a NASA U-2 airplane have shown that the strongest emission features in the cloud top optical spectra are produced by the neutral oxygen and neutral nitrogen lines in the near infrared (e.g., the OI(1) line at 777.4 nm and the NI(1) multiplet at 868.3 nm are consistently strong features).

Temporally, the optical lightning signal is comprised of a series of fast rise time, short-duration pulses associated with the energetic discharge processes occurring within the cloud. The individual pulses of cloud-to-ground lightning are generally associated with return strokes and k-changes. The optical pulse widths and rise times are highly variable and are similar for intracloud and cloud-to-ground lightning discharges; however, the interpulse intervals for intracloud flashes tend to be shorter and there are generally significantly more pulses produced during each intracloud flash.

The thundercloud is an optically thick medium and therefore strongly affects the temporal and spatial characteristics of the optical signals produced by lightning which would be observed by a satellite sensor. Although the thundercloud is optically thick, there is very little absorption at optical wavelengths. Hence, the major effect of the cloud on the optical signal is to blur the

source geometry and to delay and time-broaden the pulses due to multiple scattering. Extensive measurements from an instrumented NASA U-2 aircraft have shown that the rise time of an optical pulse is typically lengthened 150 ms and the pulses' widths tend to be 150 ms wider as a result of this multiple scattering. The median pulse rise time and the full-width-at-half-maximum obtained from the analysis of nearly 1300 pulses produced by 79 lightning flashes are 240 ms and 370 ms, respectively (Christian and Goodman, 1987).

It is important to stress that, while the cloud significantly alters the characteristics of the cloud top optical signals, the cloud does not block these emissions. When viewed from above, the optical lightning signals appear as a diffuse light source radiating from the cloud top. Measurements of the total optical energy radiated from the cloud top are in good agreement with ground-based measurements of cloud-to-ground flashes and support the theory that the cloud acts like a conservative scatterer, i.e., that most of the optical energy escapes the cloud (Christian and Goodman, 1987). Of the 79 discharges referred to above, 90% produced peak radiant energy densities of 4.7 $\mu J\ m^{-2}\ sr^{-1}$ or greater. The region of cloud top that is illuminated by a lightning flash depends on where the flash occurred within the cloud, the geometry and physical extent of the flash, and the characteristics of the cloud through which the lightning channel propagated and the radiation scattered. Theory, using Monte Carlo simulations of the radiation transfer of the optical lightning signals, and the NASA U-2 aircraft studies indicate that the diameter of the cloud top illumination associated with a single storm cell will typically be on the order of 10 km. Observations of large storm systems from the shuttle have shown that illuminated regions can exceed 60 km.

Finally, it should be noted that both intracloud and cloud-to-ground lightning flashes are readily observed from above. Extensive observations with the NASA U-2 aircraft flying over the tops of thunderstorms in coordination with ground-based measurements made under the same storms (Goodman et al., 1988a) have clearly established the viability of optical detection of all lightning. Because the majority of the channel of a cloud-to-ground flash occurs within the cloud, the light emerging from the top of the cloud has undergone a similar scattering process as an intracloud flash (the portion of the channel below cloud base is essentially undetectable from above). Further, since the scattering process dominates the characteristics of the optical signature, the optical pulses from both intracloud and cloud-to-ground flashes are very similar (Guo and Krider, 1982; Thomason and Krider, 1982; Goodman et al., 1988a). We are therefore unable to distinguish between intracloud and cloud-to-ground lightning from the optical signatures alone. While this is a limitation, it is minor because, from a scientific standpoint, it is far more important to determine the total lightning rate than either just the cloud-to-ground or intracloud rate. In fact, optical measurements of lightning from above and below the cloud will detect more return strokes than ground-based detection systems (Goodman and MacGorman, 1986; Mach et al., 1986).

2. LIS Measurement Approach

The LIS is a conceptually simple device. It images the scene much like a television camera; however, because of the transient nature of lightning, its spectral characteristics, and the difficulty of daytime detection of lightning against the brightly lit cloud background, actual data handling and processing is much different from that required by a simple imager. In order to achieve the performance goals required to meet the scientific objectives, the LIS combines off the shelf components in a unique configuration. A wide field of view lens, combined with a narrow-band interference filter is focused on a small, high speed photodiode focal plane. The signal is read out from the focal plane into a real-time data processor for event detection and

data compression. The resulting "lightning data only" signal is formatted, queued, and sent to the satellite LAN.

The particular characteristics of the sensor design results from the requirement to detect weak lightning signals during the day. During the day, the background illumination, produced by sunlight reflecting from the tops of clouds, is much brighter than the illumination produced by lightning. Consequently, the daytime lightning signals tend to be buried in the background noise, and the only way to detect lightning during daytime is to implement techniques that increase or maximize the lightning signal relative to this bright background. These techniques take advantage of the significant differences in the temporal, spatial, and spectral characteristics between the lightning signal and the background noise. A combination of four methods are employed by the LIS for this purpose. First, spatial filtering is used which matches the instantaneous field of view (IFOV) of each detector element in the LIS focal plane array to the typical cloud-top area illuminated by a lightning stroke (i.e., 5-10 km). This results in an optimal sampling of the lightning scene relative to the background illumination. Second, spectral filtering is obtained by using a narrow-band interference filter centered on a strong optical emission line (e.g., OI(1) at 777.4 nm) in the lightning spectrum. This method further maximizes the lightning signal relative to the reflected daylight background. Third, the LIS employs temporal filtering which takes advantage of the difference in lightning pulse duration of the order of 400 μs versus the background illumination which tends to be constant on the time scale of the order of seconds. In an integrating sensor, such as the LIS, the integration time specifies how long a particular pixel accumulates charge between readouts. The lightning signal-to-noise ratio improves as the integration period approaches the pulse duration. If, however, the integration period becomes too short, the lightning signal tends to be split between successive frames which actually decreases the signal-to-noise ratio. Since the median optical lightning pulse width when viewed from above is 400 ms, an integration time of 1 ms is most appropriate to minimize pulse splitting and maximize lightning detectability. Technological limitations require that a 2 ms integration time be used in the LIS instrument design; however, this compromise will not seriously degrade the sensor's performance. Even with the three "filtering" approaches discussed above, the ratio of the background illumination to the lightning signal may still exceed 50 to 1 at the focal plane. Therefore, a fourth technique, a modified frame-to-frame background subtraction, is implemented to remove the slowly varying background signal from the raw data coming off the LIS focal plane. A more detailed discussion on the measurement approach adopted for the LIS is given in Christian et al. (1989).

The real-time data processor generates an estimate of the background scene imaged at each pixel of the focal plane array. This background scene is updated during each frame readout sequence and, at the same time, the background signal is compared with the off-the-focal-plane signal on a pixel-by-pixel basis. When the difference between these signals exceeds a selected threshold, the signal is identified as a lightning event and an event processing sequence is enabled. The implementation of this real-time data processor results in a 10^5 reduction in data rate requirements while maintaining high detection efficiency for lightning events.

D. INSTRUMENT DESCRIPTION

The LIS consists of a staring imager optimized to detect and locate lightning. An imaging system, a focal plane assembly, a real-time signal processor and background remover, an event processor and formatter, power supply, and interface electronics are the six major subsystems of the sensor. The imaging system is a simple f/2 telescope consisting of a beam expander, an interference filter, and re-imaging optics. The 75° x 75° full angle LIS field of view is con-

verged to less than 5° at the interference filter in order to minimize wavelength shifts due to non-normal incidence. The focal plane assembly, including the 128 x 128 element photodiode array, preamplifiers, and multiplexers, provides subsequent electronics with a serial data stream of sufficient amplitude. As noted earlier, if after the background removal the difference signal for a given pixel exceeds a threshold, that pixel is considered to contain an event. Subsequently, the event is digitized, time tagged, location tagged, and passed to platform telemetry via the interface electronics to the satellite LAN.

1. Performance Criteria

pixel IFOV	8.5 km
FOV	75° x 75° square FOV
scene duration	180 s
wavelength	777.4 nm
threshold	4.7 J m^{-2} sr^{-1}
SNR	6
array size	128 x 128
dynamic range	>100
detection efficiency	>90% of all events
false alarm rate	<10% of total events
measurement accuracy	
location	1 pixel
intensity	10%
time	tag at frame rate
command interface	- adjust threshold - record/image - power on/off - self test - safe mode (close/open aperature cover)
weight	15 kg
power	30 watts
telemetry	
data rate	6 kb/s
format	PCM
sample size	12 bits
operating temperature	0 - 40°C

2. Imaging System

The imaging system includes a fixed focus, wide angle lens consisting of a front negative group, a telecentric beam expander used to reduce the principal ray to less than 5° where the rays go through a 1 nm bandwidth interference filter, and a rear re-imaging group behind the bandpass filter. A broad-band blocking filter is placed in front of the lens assembly in order to maximize the effectiveness of the narrow-band filter.

The need for the beam expansion optical system is driven by the incompatible requirements for a wide field of view and a narrow-band interference filter needed in order to meet signal/noise specifications. This problem occurs because the bandpass of interference filters

shifts to shorter wavelengths for non-normal incidence. That is, if the wavelength of interest is incident upon the filter at an angle that shifts it beyond the filter bandpass, the signal will not be passed. We attempt to minimize this problem by choosing a filter which passes the high wavelength end of its bandpass at normal incidence. As the angle of incidence increases to a maximum, the wavelength will shift down through the entire bandpass to the low wavelength end, allowing the use of the full filter bandwidth to compensate for the wavelength shift.

The filter temperature is tightly controlled with an active thermal heating system because the filter wavelength also changes as a function of temperature. Further, the temperature control point can be adjusted on orbit and thus, in conjunction with the optical test lamp, can be used to tune the filter if compensation becomes necessary. The telescope described above will provide a 75° x 75° full angle FOV at the focal plane with a maximum angle of incidence of 5° at the interference filter. This system has an f-number of 2, is 20 cm long, and 10 cm in diameter at its maximum width.

A lexan cover is provided in the LIS design for contamination control. This will be employed during ground processing, launch, and on-orbit operations. The cover will be transparent at 777.4 nm so that the LIS may still operate even if the aperture door fails in the closed position. A gear-driven motor will be employed for opening and closing the cover. The gear backdrive holds the cover in the open/close position.

3. Real-Time Event Processor

The need for off-the-focal plane signal processing by a real-time event processor in order to detect a lightning event has previously been addressed. Detailed electronic circuits have been designed for each of the functional elements. In addition, numerical analyses, evaluations, and trade-off options have been performed for optics and electronics.

The LIS processor extracts weak lightning flashes from an intense but slowly evolving background. The upper graph plots a given pixel's signal over one orbit. The daytime background varies with sun angle, clouds, ground albedo, etc., and can reach an excess of 500,000 electrons as compared to signal electrons which may be as small as 5000 electrons. A lightning stroke occurs during a single frame producing a signal that is superimposed on top of the essentially constant background. The real-time processor continuously averages the output from the focal plane over a number frames on a pixel-by-pixel basis in order to generate a background estimate. It then subtracts the average background estimate from the current signal.

The subtracted signal consists of shot noise fluctuating about a zero with occasional peaks due to lightning events. When a peak exceeds the level of the variable threshold, it is considered to be a lightning event and is processed by rest of the circuit. The threshold must be set sufficiently high that false triggers are kept to a small percent of the total lightning rate. Clearly, the threshold must be higher during daytime when shot noise is dominated by the solar background.

The components of the real-time event processor include a background signal estimator, a background remover, a lightning event thresholder, an event selector, and a signal identifier. Analog/digital hybrid processing is used in a unique way in that it takes advantage of the strengths of each technology in order to provide high processing rates while consuming minimal power. Much of the signal processing is performed in a pipeline fashion that maximizes throughput.

The background estimator (averager) and remover (subtracter) circuits combine to perform the functions of a time domain low pass filter. The signal coming off the focal plane is fed through a buffer and clipping stage in order to ensure that a strong lightning signal does not contaminate the background estimate. The signal is then multiplied by a fractional gain (B) and

added to (1-B) times the previous background estimate for the same pixel. The inverse of the fractional gain is equivalent to the number of frames used in generating the background estimate and is analogous to setting the cutoff frequency in conventional frequency domain filters. Too high a fractional gain might permit lightning events to contaminate low background estimates and would increase the processing noise. Too low a fractional gain would not allow the background estimator to respond rapidly enough to changes in background intensity. In the baseline design, 1/B is set to six.

The proper operation of the background estimator requires that the background data are clocked through the estimator synchronously with the data being clocked off the focal plane and that the number of discrete storage elements in the background memory is exactly the same as the number of pixels in the focal plane array. When data are properly synchronized, the signal appearing on the output of the delay line during a given clock cycle corresponds spatially to the signal being clocked off the focal plane. That is, it contains a history of what that specific pixel has measured over the last 1/B frames. These two signals are then be subtracted using a difference amplifier in order to generate a difference signal. Since the original signal contains either background plus lightning or just background, the subtracted signal will be either a lightning signal, near zero, or a false alarm as previously described.

The difference signal is then compared with the threshold level (which may be adaptive). If the signal exceeds the threshold level, a comparator triggers, which enables a switch and passes the lightning signal for further processing. In addition, the comparator output is encoded using a digital multiplexer in order to generate a row address that identifies the specific pixel that detected the lighting event. The digital outputs from the data processor represent the intensity of the lighting event and the location where the lightning occurred. These signals are then forwarded to encoding electronics in which the data are formatted into a digital bit stream and sent to the platform LAN.

II. DATA PRODUCTS

A. LIS DATA DESCRIPTION

At a frame rate of about 2 ms, the data rate coming off the LIS focal plane multiplexer is about 8 million samples per second. However, only a small portion of the data coming off the focal plane contains information on lightning events; most contains only background signal which is removed by an onboard real-time event processor on a pixel-by-pixel basis. The real-time event processor subtracts the background running average from the signal coming off the focal plane assembly and compares the result to a threshold. If the difference exceeds the threshold, the signal is digitized (i.e., an event detected). The threshold level can be adjusted from the ground to increase LIS sensitivity during night imaging. The implementation of this real-time processor to detect lightning events against background noise will reduce the data rate by a factor greater than 10^5.

Once the optical pulse radiance data have been digitized they will be combined with pixel location coordinates and stored in an internal buffer. The data are then formatted and assembled into a packet for delivery to the on board storage system via the LAN for later telemetry to the ground. The packet will consist of a header specifying the instrument of origin, destination, and engineering data followed by the LIS science data. Generally, a frame will not be transmitted when the frame does not contain pixels that exceed the threshold value for lightning detection.

LIS data will not tax the Earth Probe LAN or data storage system. During maximum data rates, for example, while the sensor is overlooking a large thunderstorm system (e.g., an extremely active mesoscale convective complex), aircraft (U-2, ER-2) and ground-based studies indicate that the maximum lightning event rate within the LIS field of view will be no more than 75 pulses per second. This corresponds to a data rate of no more than 3 kbits in one second (data rate for the LIS will be no more than 6 kbits s^{-1}). Furthermore, at least 98% of the time the LIS will not be detecting lightning and will only broadcast a message to indicate that the instrument is operational. The onboard storage requirements of the LIS data will also be simple.

The lightning sensor will accept a few simple commands from the ground. These commands will be used infrequently, but are provided to cover almost all possible situations. The commands will include the ability to turn on the instrument or put it into a sleep mode, to obtain an image of the surface (rather than the difference signal) for calibration, maintenance, and navigation purposes, to adjust the event detection threshold, and to provide a check of the system performance and health and report the results.

B. STANDARD DATA PRODUCTS

This section describes the standard data products that will be produced and archived in the MSFC DAAC. It is anticipated at this time that all of the standard data products from level 1A to level 3 (and higher levels if they are later developed) will be permanently archived. Scientific investigations will probably only routinely employ levels 1A, 2, and 3 data products.

1. Level 0 Data

Level 0 data products can be defined as raw instrument data at original resolution, time ordered, with duplicates removed. The message part of the LIS packet transmission will constitute the level 0 data without further processing.

2. Level 1 Data

The level 1 data products consist of the level 0 data products packed with georeferencing information and ancillary data. This intermediate LIS product will also include a time stamp computation and calibration information appended to the level 0 data product.

3. Level 1A Data

The level 1A data products are transformed values of full resolution instrument measurements. The data will consist of an individual optical pulse with Universal Time of origin, latitude and longitude of source, radiance of pulse and threshold setting. These products will be used for studying individual lightning events at highest time resolution. All higher level standard data products will be derived from level 1A data products.

4. Level 2 Data

The data at this level consist of geophysical parameters located in space and time. The polar orbit limits the time of continuous observation for any point within the field of view to about 3 minutes. The level 2 data products are obtained by combining level 1A data for individual events at a particular location for an observation period. Algorithms will be used to identify adjacent pixels illuminated by the same event (i.e., a single optical lightning pulse may illuminate more than one pixel). Additional analysis of the optical pulse data will be performed to identify individual lightning flashes. Optically, a single lightning flash is comprised of a series of discrete short-duration optical pulses associated with energetic discharge processes occurring within the cloud. Of course, it is recognized that not all the optical events in a flash will exceed the LIS threshold and be detected.

Level 2 data products will include complete geophysical parameters of the total pulses and lightning flashes occurring in an observation period. Depending on advances in ongoing research, the flashes may be further distinguished by type of discharge (i.e., whether cloud-to-ground or intracloud discharge). Because of a significant difference between day and night thunderstorm activities, it is anticipated that two sets of data will be produced. Level 3 data products will be derived from the level 2 data products.

5. Level 3 Data

The level 3 data products consist of LIS geophysical parameters mapped and time averaged onto a uniform Earth based grid. The spatial resolution of the grids can be as small as about 0.1° since this represents the approximate pixel resolution for the LIS instrument. Standard level 3 data products will be produced with spatial resolution between 0.1° and 2.5° The data will be accumulated to produce global pentads, monthly, seasonal, yearly, annual and interannual maps of lightning. Level 3 data products will include maps and/or statistics of total optical pulses, total flashes, densities, radiant intensities, discharge type, and flash duration as well as mean and extreme value statistics.

C. SPECIALIZED DATA PRODUCTS

1. Storm and Storm Complex Identification

This product will be derived from the level 2 data. The standard data product produces information on individual lightning flashes during an observation period. This specialized product will be produced by applying clustering algorithms to identify individual storm cells and storm complexes (e.g., organized convection associated with fronts, squall lines, mesoscale convective complexes, etc.). Since lightning is closely associated with vigorous convection, this product will help document the distribution, intensity, and climatic variability of global convection, particularly in the data-sparse tropics and oceanic regions of the Earth. This product will provide a diagnostic parameter (i.e., lightning) that will undoubtably improve estimates of convective precipitation that rely on satellite passive microwave, infrared, and other remote sensing measurements (e.g., SSM/I, AVHRR, GOES data). It is quite likely that this specialized product as it is perfected and automated will become a standard data product designated as level 4.

2. Empirical Relationships

Several topics of geophysical interest are closely related to lightning and thunderstorms. Lightning is a global phenomenon that can be used as a measure of some of the variables in global change. Lightning activity is associated with thunderstorms that produce heavy rainfall in many climatic regions and, therefore, can be used to increase our knowledge of the distribution, structure, and variability of thunderstorms at the local, regional, and global scale over the land and ocean. Atmospheric teleconnections due to ENSO (El Nino Southern Oscillation) and anti-ENSO events in the tropical Pacific often result in significant changes in the frequency and movement of storm tracks and precipitation patterns. These climate variations will also produce changes in lightning activity in both the northern and southern hemispheres. Lightning is also one of the major sources of naturally occurring NO_x and other trace gases such as ozone (O_3), and thunderstorms maintain the Earth's electric circuit. Again note, lightning measurements are simple to make and produce small data sets for storage and analysis.

In all the investigations, an emphasis will be placed on establishing quantitative relationships that could employ lightning data, such as will be derived from the LIS observations, as the independent variable. Already, empirical relationships have been found relating lightning to precipitation and to storm electric current output. As research continues, the existing empirical relationships, which form the basis for the specialized data products, will be improved and refined and other relationships (e.g., in the area of atmospheric trace gas chemistry) will be developed.

D. LIS DATA FLOW FOR EOS

Figure 10 illustrates the major data flows in the LIS program. The LIS will transmit raw (i.e., level 0) data that will be forwarded to the MSFC DAAC. At the MSFC DAAC, the level 0 LIS data will be processed with ancillary EOS navigation and engineering data in the Product Generation Facility (PGF) to produce standard data products as described in section II.B. The Science Computing Facility will access LIS data from the MSFC DAAC and from numerous other sources as illustrated in Figure 10 for algorithm development, LIS data validation, and scientific data analysis and research. We expect to provide a similar capability for TRMM.

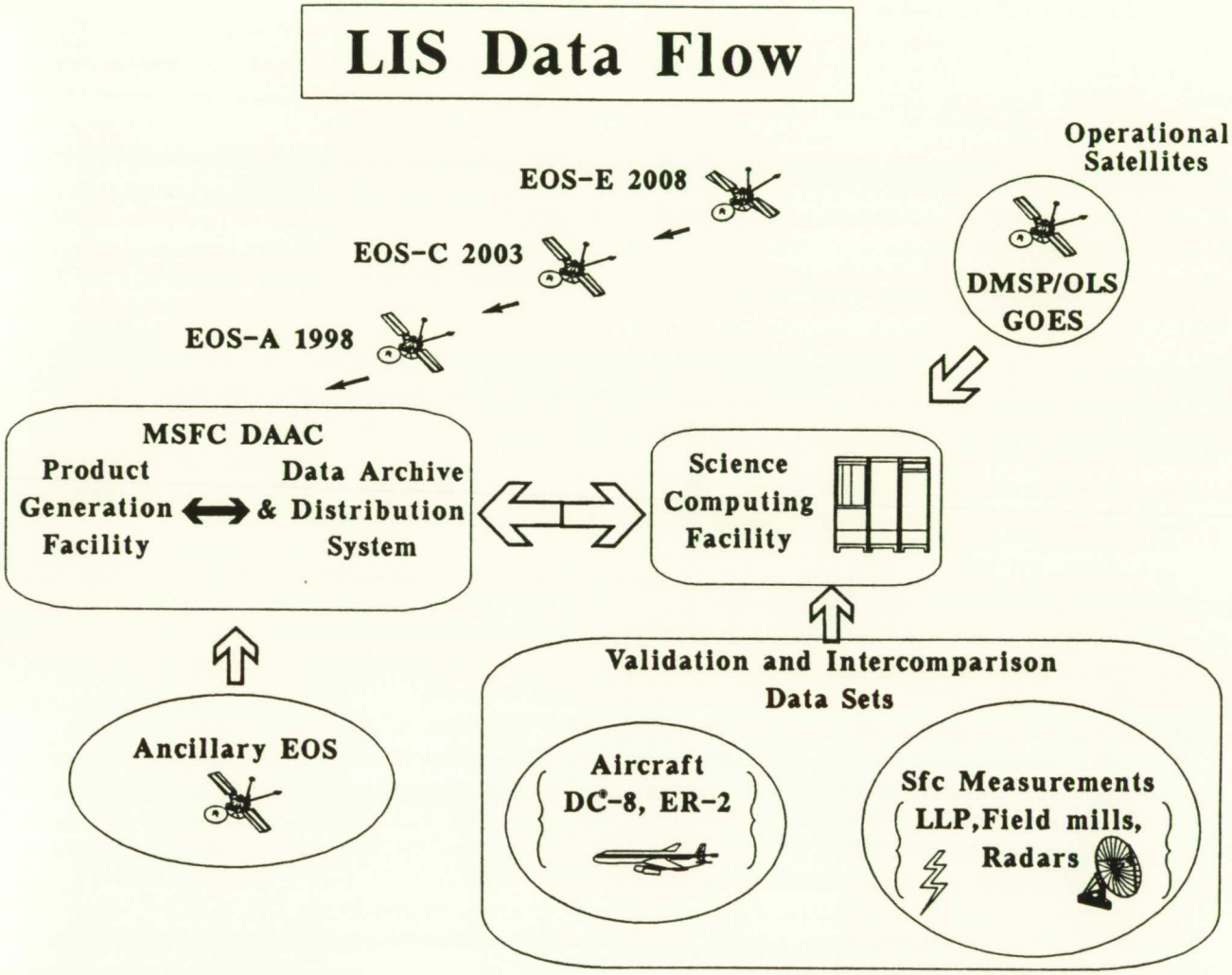

Fig. 10. LIS Data Flow.

REFERENCES

Barrett, E.C., and D.W. Martin, 1981. The Use of Satellite Data in Rainfall Monitoring, Academic Press, New York, 340 pp.

Battan, L. J., 1965. Some factors governing precipitation and lightning for convective clouds, J. Atmos. Sci., 22, 79.

_____, 1967. Cloud seeding and cloud-to-ground lightning, J. Appl. Meteor., 6, 102.

Bjerknes J., 1969. Atmospheric teleconnections from the equatorial Pacific, Mon. Wea. Rev., 97, 163.

Blakeslee, R. J., H. J. Christian, and B. Vonnegut, 1989. Electric measurements over thunderstorms , J. Geophys. Res., 94, 13135-13140.

Braham, R. R., 1952. The water and energy budgets of the thunderstorm and their relation to thunderstorm development, J. Meteor., 9, 227.

Buechler, D. E., and S. J. Goodman, 1990. Echo size and asymmetry: Impact on NEXRAD storm identification, J. Appl. Met., 29, 962-969.

Byers, H. R., 1974. General Meteorology, McGraw Hill, Inc., New York, 306.

_____, and R.R. Braham, Jr., 1949. The Thunderstorm, U.S. Govt. Printing Office, Washington, D.C.

Chameides, W. L., D. D. Davis, J. Bradshaw, M. Rodgers, S. Sandholm, and D. B. Bai, 1987. An estimate of NO_x production in electrified clouds based on NO estimates from the GTE CITE 1 fall 1983 field operation, J. Geophys. Res., 92, 2153-2156.

_____,1986. The role of lightning in the chemistry of the atmosphere, in The Earth's Electrical Environment, National Academy Press, 70-77.

Chen, T., 1987. Comments on "Global distribution of midnight lightning: September 1977 to August 1978," Mon. Wea. Rev., 115, 3202.

Christian, H. J., R. L. Frost, P. H. Gillaspy, S. J. Goodman, O. H. Vaughn, M. Brook, B. Vonnegut, and R. E. Orville, 1983. Observations of optical lightning emissions from above thunderstorms using U-2 aircraft, Bull. Am. Meteor. Soc., 64, 120.

_____, W. W. Vaughn, and J. C. Dodge, 1984. A technique for the detection of lightning from geostationary orbit, Preprints, 7th Int. Conf. Atmos. Elect., Albany, New York, 452.

_____ and S. J. Goodman, 1987. Optical observations of lightning from a high altitude airplane, J. Atmos. Ocean. Tech., 4, 701.

_____, R. J. Blakeslee, and S. J. Goodman, 1989. The detection of lightning from geostationary orbit, J. Geophy. Res., 94, 13329-13337.

Christy, J. R., 1991. Diabatic heating rate estimates from ECMWF analyses, J. Geophys. Res., 96, 5123-5135.

Cornejo-Garrido, A. G. and P. H. Stone, 1977. On the heat balance of the Walker Circulation, J. Atmos. Sci., 34, 1155.

Drapcho, D.L., D. Sisterson, and R. Kumar, 1983. Nitrogen fixation by lightning activity in a thunderstorm, Atmos. Environ., 17, 729-734.

Eaton, L. R., C. W. Poon, J. C. Shelton, N. P. Loverty, and R. D. Cook, 1983. Lightning mapper sensor design study, NASA CR-170909, Marshall Space Flight Center, AL.

Franzblau, E and C. J. Popp, 1989. Nitrogen oxides produced from lightning, J. Geophys. Res., 94, 11089-11104.

Fritsch, J. M., T. T. Warner, N. L. Seaman, H. Chang, and D. Zhang, 1986. A case study of the sensitivity of numerical simulation of mesoscale convective systems to varying initial conditions, Mon. Wea. Rev., 114, 2418.

Goodman, S. J., and D. R. MacGorman, 1986. Cloud-to-ground lightning activity in mesoscale convective complexes, Mon. Wea. Rev., 114, 2320.

_____, H. J. Christian, and W. D. Rust, 1988a. Optical pulse characteristics of intracloud and cloud-to-ground lightning observed from above clouds, J. Appl. Meteor., 27, 1369-1381.

_____, D. E. Buechler, P. D. Wright, and W. D. Rust, 1988b. Lightning and precipitation history of a microburst producing storm, Geophys. Res. Lett., 15, 1185-1188.

_____, _____, and P. J. Meyer, 1988c. Convective tendency images derived from a combination of lightning and satellite data, Weather and Forecasting, 3, 173-188.

_____, D. E. Buechler, P. D. Wright, W. D. Rust, and K. E. Nielsen, 1989. Polarization radar and electrical observations of microburst producing storms during COHMEX, Preprints, 24th Conf. on Radar Meteorology, Tallahassee, FL, Mar. 27-31, Amer. Meteor. Soc., Boston.

_____, and _____, 1990. Lightning-Rainfall Relationships, Preprints, Conf. on Operational Precipitation Estimation and Prediction, Anaheim, CA, Feb. 7-9, Amer. Meteor. Soc., Boston.

_____, and H. J. Christian, 1992. Lightning. To appear as chapter in Global Change Atlas, R. Gurney, J. Foster, and C. Parkinson, eds., Cambridge University Press, New York.

Grosh, T., 1978. Lightning and precipitation - The life history of isolated thunderstorms, Preprints, Conf. Cloud Phys. Atm. Electricity, Issaquah, WA, Am. Meteor. Soc., Boston, MA, 617.

Guo, C. and E. P. Krider, 1982. The optical and radiation field signatures produced by lightning return strokes, J. Geophys. Res., 87, 8913.

Herman, J. R., J. A. Caruso, and R. G. Stone, 1965. Radio astronomy explorer (RAE)-1, observation of terrestrial radio noise, Planet. Space Sci., 21, 443.

Holton, J. R., 1972. An Introduction to Dynamic Meteorology, Academic Press, New York, New York, 279.

Holzworth, R. H. and Y. T. Chiu, 1982. Sferics in the stratosphere, CRC Handbook of Atmospherics, Vol. 2, H. Volland, ed., 1.

Horner, F. and R. B. Bent, 1969. Measurements of terrestrial radio noise, Proc. Roy. Soc. A, 311, 527.

Houze, R. A. and A. K. Betts, 1981. Convection in GATE, Rev. Geophys. Space Phys., 19, 541.

Janowiak, J. E., and P. A. Arkin, 1990. Rainfall variations in the tropics during 1986-1989, J. Geophys. Res., submitted.

Kinzer, G. D., 1974. Cloud-to-ground lightning versus radar reflectivity in Oklahoma thunderstorms, J. Atmos. Sci., 31, 787-799.

Kotaki, M. and C. Katoh, 1983. The global distribution of thunderstorm activity observed by the ionosphere sounding satellite (ISS-b), J. Atm. Terr. Phys., 45, 833.

Levine, J. S. and E. F. Shaw, 1983. In situ aircraft measurements of enhanced levels of N_2O associated with thunderstorm lightning, Nature, 303, 312.

Lindzen, R. S. and S. Nigam, 1987. On the role of sea surface temperature gradients in forcing low-level winds and convergence in the tropics, J. Atmos. Sci., 44, 2418.

Livingston, J. M. and E. P. Krider, 1978. Electric fields produced by Florida thunderstorms, J. Geophys. Res., 83, 385.

Mach, D. M., D. R. MacGorman, W. D. Rust, and R. T. Arnold, 1986. Site errors and detection efficiency in a magnetic direction-finder network for locating lightning strikes to ground, J. Atmos. Ocean. Tech., 3, 67.

NASA, 1990. Global Tropospheric Experiment: Probing the Chemistry/Climate Connection, Available from NASA Headquarters, Code SEU, Washington, D.C. 20546.

Neelin, J. D. and I. M. Held, 1987. Modeling tropical convergence based on the moist static energy budget, Mon. Wea. Rev., 115, 3.

Norwood, V., 1983. Lightning mapper sensor study, NASA CR-170908, Marshall Space Flight Center, AL.

Noxon, J. A., 1976. Atmospheric nitrogen fixation of lightning, Geophys. Res. Lett., 3, 463-465.

_____, 1978. Tropospheric NO_2, J. Geophys. Res., 83, 3051-3057.

Olson, W. S., F. J. LaFontaine, W. L. Smith, and T. H. Achtor, 1990. Recommended algorithms for the retrieval of rainfall rates in the tropics using the SSM/I (DMSP-8), IEEE Transactions on Geoscience and Remote Sensing, submitted.

Orville, R. E., 1982. Lightning detection from space, CRC Handbook of Atmospherics, Vol. 2, H. Volland, ed., 79.

_____ and R. Henderson, 1984. Absolute spectral irradiance measurements of lightning from 375 to 880 nm, J. Atmos. Sci., 41, 3180.

_____ and _____, 1986. Global distribution of midnight lightning: September 1977 to August 1978, Mon. Wea. Rev., 114, 2640.

Piepgrass, M. V., E. P. Krider, and C. B. Moore, 1982. Lightning and surface rainfall during Florida thunderstorms, J. Geophys. Res., 87, 11193.

Price, C., and D. Rind, 1990. The effect of global warming on lightning frequencies, Preprints, 16th Conf. on Severe Local Storms, Oct. 22-26, Kananaskis Park, Alberta, Canada, Am. Meteor. Soc., Boston, 748-751.

Rasmussen, E. M. and T. H. Carpenter, 1982. Variations in tropical sea surface temperatures and surface wind fields associated with the Southern Oscillation/El Nino, Mon. Wea. Rev., 110, 354.

Reynolds, S. E., and M. Brook, 1956. Correlation of the initial electric field and the radar echo in thunderstorms, J. Meteor., 13, 376-380.

Riehl, H. and J. S. Malkus, 1958. On the heat balance in the equatorial trough zone, Geophysica, 6, 503.

Robertson, F. R., G. S. Wilson, H. J. Christian, S. J. Goodman, G. H. Fichtl, and W. W. Vaughan, 1984. Atmospheric science experiments applicable to space shuttle spacelab missions, Bull. Am. Meteor. Soc., 65, 692.

Shackford, C. R., 1960. Radar indications of a precipitation-lightning relationship in New England thunderstorms, J. Meteor., 17, 15-19.

Sparrow, J. G. and E. P. Ney, 1971. Lightning observations by satellite, Nature, 232, 540.

Thomason, L. W. and E. P. Krider, 1982. The effects of clouds on the light produced by lightning, J. Atmos. Sci., 39, 2051.

Turman, B. N., 1978. Analysis of lightning data from the DMSP satellite, J. Geophys. Res., 83, 5019.

_____, 1979. Lightning detection from space, Am. Sci., 67, 321.

_____ and R. J. Tettelbach, 1980. Synopic-scale satellite lightning observations in conjunction with tornadoes, Mon. Wea. Rev., 108, 1978.

Vonnegut, B., O. H. Vaughan, and M. Brook, 1983. Photographs of lightning from the space shuttle, Bull. Am. Meteor. Soc., 64, 150.

Vorpahl, J. A., J. G. Sparrow, and E. P. Ney, 1970. Satellite observations of lightning, Science, 169, 860.

Williams, E. P., 1985. Large-scale charge separation in thunderstorms, J. Geophys. Res., 90, 6013.

_____, and S. A. Rutledge, 1990. Studies of electrification and lightning in deep tropical precipitation systems, Preprints, AMS Conf. on Cloud Physics, San Francisco, CA, July 23-27, Amer. Meteor. Soc., Boston, 5 pp.

_____, S. A. Rutledge, S. G. Geotis, N. Renno, E. Rasmussen, and T. Rickenback, 1991. A radar and electrical study of tropical "hot towers," J. Atmos. Sci., in press.

Wilson, C. T. R., 1920. Investigations on lightning discharges and on the electric field of the Earth, Phil. Trans. Roy. Soc. London, A221, 73.

Workman, E. J. and S. E. Reynolds, 1949. Electrical activity as related to thunderstorm cell growth, Bull. Am. Meteor. Soc., 30, 142.

Zawadzki, I., E. Torlaschi, and R. Sauvageau, 1981. The relationship between mesoscale thermodynamic variables and convective precipitation, J. Atmos. Sci., 38, 1535-1540.

REPORT DOCUMENTATION PAGE

Form Approved
OMB No. 0704-0188

1. AGENCY USE ONLY *(Leave blank)*	2. REPORT DATE	3. REPORT TYPE AND DATES COVERED
	February 1992	**Technical Memorandum**

4. TITLE AND SUBTITLE

Lightning Imaging Sensor (LIS) for the Earth Observing System

5. FUNDING NUMBERS

6. AUTHOR(S)

Hugh J. Christian, Richard J. Blakeslee, and Steven J. Goodman

7. PERFORMING ORGANIZATION NAME(S) AND ADDRESS(ES)

George C. Marshall Space Flight Center
Marshall Space Flight Center, AL 35812

8. PERFORMING ORGANIZATION REPORT NUMBER

M-680

9. SPONSORING / MONITORING AGENCY NAME(S) AND ADDRESS(ES)

National Aeronautics and Space Administration
Washington, D.C. 20546

10. SPONSORING / MONITORING AGENCY REPORT NUMBER

NASA TM-4350

11. SUPPLEMENTARY NOTES

Prepared by Space Science Laboratory, Science & Engineering Directorate.

12a. DISTRIBUTION / AVAILABILITY STATEMENT

Unclassified—Unlimited

Subject Category: 43

12b. DISTRIBUTION CODE

13. ABSTRACT *(Maximum 200 words)*

This document describes scientific objectives and instrument characteristics of a calibrated optical Lightning Imaging Sensor (LIS) for the Earth Observing System (EOS) and the Tropical Rainfall Measuring Mission (TRMM) designed to acquire and investigate the distribution and variability of total lightning on a global basis. The LIS is an EOS instrument, whose lineage can be traced to a lightning mapper sensor planned for flight on the GOES series of operational meteorological satellites. The LIS is conceptually a simple device, consisting of a staring imager optimized to detect and locate lightning. The LIS will detect and locate lightning with storm scale resolution (i.e., 5-10 km) over a large region of the Earth's surface along the orbital track of the satellite, mark the time of occurrence of the lightning, and measure the radiant energy. The LIS will have a nearly uniform 90% detection efficiency within the area viewed by the sensor, and will detect intracloud and cloud-to-ground discharges during day and night conditions. In addition, the LIS will monitor individual storms and storm systems long enough (i.e., 2 minutes) to obtain a measure of the lightning flashing rate in these storms when they are within the field of view of the LIS. The LIS attributes include low cost, low weight and power (15 kg, 30 watts), low data rate (6 kb/s), and important science. The LIS will contribute to studies of the hydrological cycle, general circulation and sea-surface temperature variations, investigations of the electrical coupling of thunderstorms with the ionosphere and magnetosphere, and observations and modeling of the global electric circuit. It will provide a global lightning climatology from which changes, caused perhaps by subtle temperature variations, will be readily detected.

14. SUBJECT TERMS	15. NUMBER OF PAGES
Satellite Meteorology, Remote Sensing, Lightning, Thunderstorms, Earth Observing System (EOS), Tropical Rainfall Measuring Mission (TRMM)	44
	16. PRICE CODE A03

17. SECURITY CLASSIFICATION OF REPORT	18. SECURITY CLASSIFICATION OF THIS PAGE	19. SECURITY CLASSIFICATION OF ABSTRACT	20. LIMITATION OF ABSTRACT
Unclassified	**Unclassified**	**Unclassified**	**Unlimited**

National Aeronautics and
Space Administration
Code NTT-4

Washington, D.C.
20546-0001